

Geomorphologic controls and anthropogenic impacts on dissolved organic carbon from mountainous rivers: Insights from optical properties and carbon isotopes

Shuai Chen¹, Jun Zhong², Lishan Ran¹, Yuanbi Yi², Wanfa Wang³, Zelong Yan⁴, Si-liang Li^{2,5}, Khan M.G. Mostofa²

¹Department of Geography, The University of Hong Kong, Pokfulam Road, Hong Kong, China

²Institute of Surface-Earth System Science, School of Earth System Science, Tianjin University, Tianjin, 300072, China

³College of Resources and Environmental Engineering, Key Laboratory of Karst Georesources and Environment, Ministry of Education, Guizhou University, Guiyang, 550025, China

⁴School of Environmental Science and Technology, Dalian University of Technology, Dalian, 116081, China

⁵State Key Laboratory of Hydraulic Engineering Simulation and Safety, Tianjin University, Tianjin 300072, China

Correspondence to: Jun Zhong (jun.zhong@tju.edu.cn) and Lishan Ran (lsran@hku.hk)

Abstract. Mountainous rivers are critical in transporting dissolved organic carbon (DOC) from terrestrial environments to downstream ecosystems. However, how geomorphologic factors and anthropogenic impacts control the composition and export of DOC in mountainous rivers remains largely unclear. Here, we explore DOC dynamics in three subtropical mountainous catchments (i.e., the Yinjiang, Shiqian, and Yuqing catchments) in southwest China which are heavily influenced by anthropogenic activities. Water chemistry, stable and radioactive carbon isotopes of DOC ($\delta^{13}\text{C}_{\text{DOC}}$ and $\Delta^{14}\text{C}_{\text{DOC}}$), and optical properties (UV absorbance and fluorescence spectra) were employed to assess the biogeochemical processes and controlling factors on riverine DOC. The radiocarbon ages of DOC in the Yinjiang River varied widely from 928 years before present to modern. Stepwise multiple regression analyses and partial least square path models revealed that geomorphology and anthropogenic activities were the major drivers controlling DOC concentrations and DOM characteristics. Catchments with higher catchment slope gradients were characterized by lower DOC concentrations, enriched $\delta^{13}\text{C}_{\text{DOC}}$ and $\Delta^{14}\text{C}_{\text{DOC}}$, and more aromatic dissolved organic matter (DOM), which were opposite to those with gentle catchment slopes. Variabilities in DOC concentrations were also regulated by land use with higher DOC concentrations in urban and agricultural areas. Furthermore, DOM in catchments with a higher proportion of urban and agricultural land uses was less aromatic, less recently produced and exhibited a higher degree of humification and more autochthonous humic-like DOM. This research highlights the significance of incorporating geomorphologic controls on DOC sources and anthropogenic impacts on DOM composition into the understanding of DOC dynamics and quality of DOM in mountainous rivers which are globally abundant.

1 Introduction

Dissolved organic carbon (DOC) plays a fundamental role in the riverine carbon cycle with approximately 0.26 Pg (1Pg

32 =10¹⁵g) of DOC exported from global rivers to the ocean each year, accounting for more than half of the total organic carbon
33 export (Cai, 2011; Raymond and Spencer, 2015). Owing to continued climate warming and rapid land use changes, it is
34 important to gain a better understanding of the spatial and temporal dynamics of DOC transport in river systems (Butman et
35 al., 2014; Fasching et al., 2016; Zhong et al., 2021). For example, the elevated temperature has a dominant effect on DOC
36 concentration and dissolved organic matter (DOM) composition by enhancing decomposition and photochemical
37 degradation rates of DOM (Zhou et al., 2018), contributing to significant CO₂ emissions from inland waters (Raymond et al.,
38 2013). Additionally, DOM provides energy and nutrient sources for aquatic biota (Findlay et al., 1998), adsorbing heavy
39 metals and organic pollutants (Aiken et al., 2011). Riverine DOC can also restrict in-stream primary production by reducing
40 light penetration and lowering temperature in the water column, thereby serving as an important determinant in shaping the
41 ecological and biogeochemical processes in aquatic environments (Ask et al., 2009). Therefore, disentangling the processes
42 controlling riverine DOC dynamics is crucial for a greater understanding of aquatic ecosystem functioning and the global
43 carbon cycle. Recent advances in spectroscopic techniques, especially the UV-visible spectrophotometry and fluorescence
44 spectroscopy, and widespread application of stable and radioactive carbon isotopes on bulk DOC have provided insights into
45 the composition, source, and age of DOM in freshwater ecosystems (Fellman et al., 2010; Marwick et al., 2015; Minor et al.,
46 2014). These new techniques have led to significant improvements in our understanding of the biogeochemical processes of
47 DOC in river systems, which will continue to be effective tools for researchers to gain deeper insights into the riverine
48 carbon cycle.

49 The biogeochemical processes of DOM in river systems have been extensively studied, which depend largely on the
50 sources and composition of DOM (Toming et al., 2013). Riverine DOM is a mixture generated from autochthonous and
51 allochthonous sources. Among them, autochthonous DOM is a pool of dead and living microbial and algal biomass that is
52 derived within the aquatic ecosystem (Devesa-Rey and Barral, 2011), which mainly consists of non-humic substances that
53 are more bioavailable (Toming et al., 2013). In comparison, allochthonous DOM refers to DOM that originates from outside
54 of the aquatic ecosystem and is typically composed of higher plants and soil organic matter (Zhang et al., 2023), which may
55 also contain organic waste of anthropogenic origin (Ramos et al., 2006; Toming et al., 2013). Consequently, allochthonous
56 DOM is generally characterized by high lignin content and high molecular weight, making it refractory to decomposition
57 (Devesa-Rey and Barral, 2011).

58 Recent studies have indicated the significance of geomorphologic factors, such as elevation and catchment slope, in
59 influencing the export of DOC and riverine carbon cycling (Connolly et al., 2018; Li Yung Lung et al., 2018). Compared
60 with high-relief catchments, low relief regions with longer water residence time, stronger hydrologic connectivity to rivers,
61 and greater development of wetlands are typically characterized by increased concentration of riverine DOC (Harms et al.,
62 2016; McGuire et al., 2005). A recent global study on lakes and rivers found that increasing elevation is associated with

63 greater protein-like fluorescent DOM and lower specific ultraviolet absorbance at 254 nm (SUVA₂₅₄), which indicates the
64 effect of enhanced UV radiation and accumulation of autochthonous DOM in higher elevation areas (Zhou et al., 2018).
65 More specifically, DOC supply is likely regulated by the amount of stored soil organic carbon (SOC) in a catchment (Lee et
66 al., 2019; Rawlins et al., 2021). However, this supply is limited by shallow soil depth and high flow velocity (Lee et al.,
67 2019). The varying extent of hydrologic connectivity due to changing water residence time with different catchment slopes
68 may also have significant influences on DOC dynamics (Connolly et al., 2018). Typically, it is anticipated that as the slope
69 increases towards higher elevation areas, where residence time is relatively short and soil organic matter is well-connected to
70 hydrologic pathways, the composition of DOM pools in inland waters will shift towards a more “terrestrial” characteristic.
71 This shift involves larger molecules with high molecular weight and aromatic structures (Creed et al., 2018; Xenopoulos et
72 al., 2021). Although geomorphologic characteristics have proved to be useful in estimating DOC concentrations (Harms et
73 al., 2016; Mzobe et al., 2020), the underlying mechanisms that regulate DOC dynamics in small mountainous rivers remain
74 poorly understood. Therefore, a deep understanding of the geomorphologic controls on DOC dynamics is urgently needed.
75 Subtropical small mountainous rivers are characterized by steep catchment slopes, high erosion rates, frequent rainfall events
76 in wet seasons, and rapid change in hydrology during these rainfall events (Lee et al., 2019; Leithold et al., 2006), yet have
77 received little research attention regarding their DOC dynamics. Moreover, runoff, catchment slope gradient, and SOC have
78 been recognized as good predictors for DOC export in small mountainous rivers (Lee et al., 2019). Yet, the extent to which
79 these factors, along with land use patterns, effectively regulate the DOC dynamic is still far from well-understood (Lee et al.,
80 2019; Moyer et al., 2013).

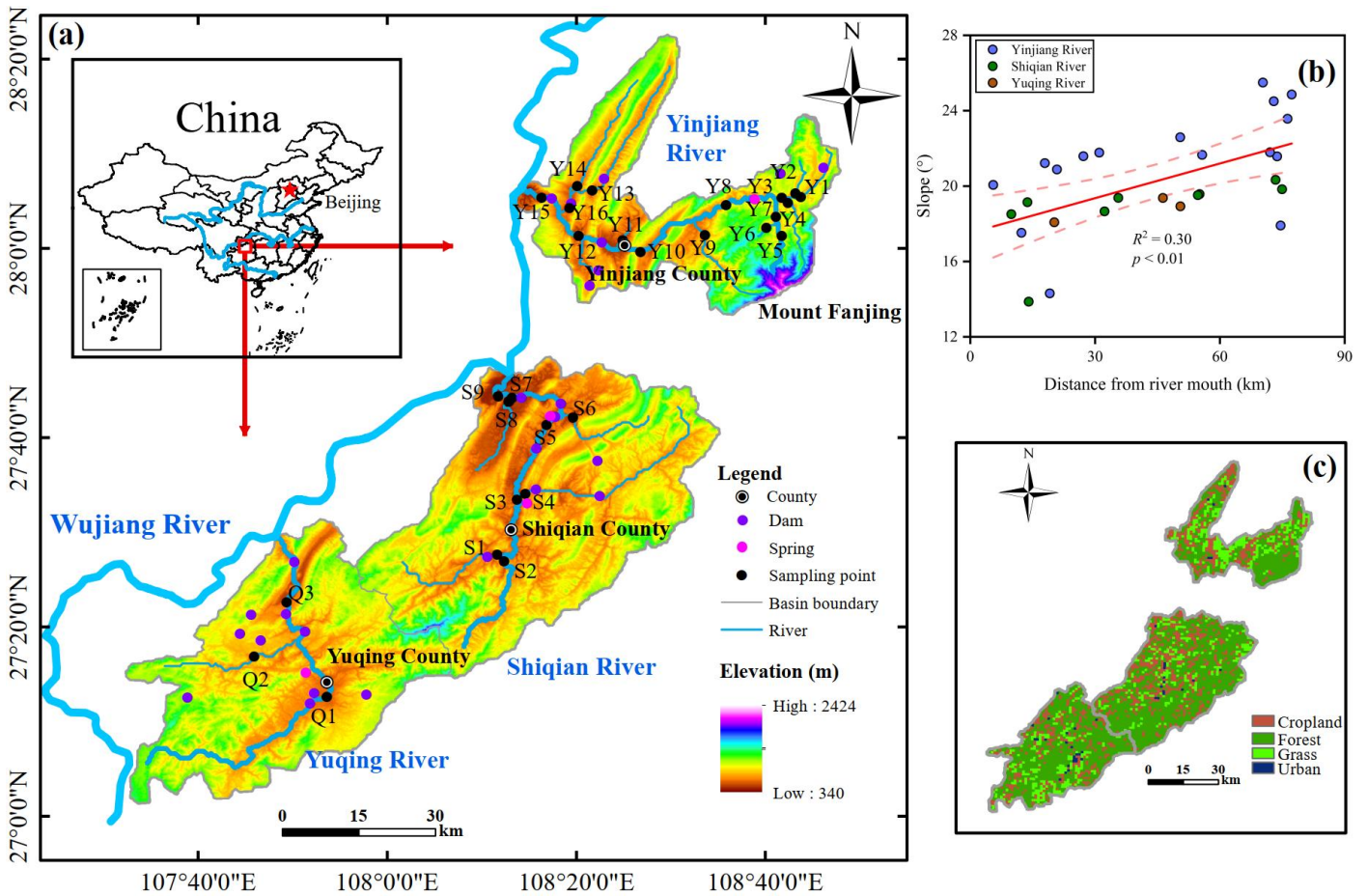
81 Anthropogenic impacts, such as urban and agricultural land uses, have led to significant alterations to the flux of DOC
82 and the fate and quality of DOM in global streams and rivers (Coble et al., 2022; Wilson and Xenopoulos, 2008; Xenopoulos
83 et al., 2021). Agricultural streams and rivers are dominated by microbial-derived, protein-like DOM, while urban freshwater
84 ecosystems are characterized by microbial, humic-like or protein-like, and autochthonous DOM (Hosen et al., 2014;
85 Williams et al., 2016; Xenopoulos et al., 2021). Agricultural and urban land uses tend to increase nutrient loading in streams,
86 resulting in enhanced bacterial production and DOM decomposition (Quinton et al., 2010; Williams et al., 2010). As a result,
87 microbial-derived DOM plays a crucial role in agricultural and urban rivers. In addition, DOM tends to have a more reduced
88 redox state and is likely more labile and accessible to the microbial community in agricultural streams when compared to the
89 DOM found in natural streams (Fasching et al., 2019; Williams et al., 2010). On the scale of years to decades, anthropogenic
90 impacts can accelerate terrestrially sourced DOC export to aquatic ecosystems (Xenopoulos et al., 2021). On the scale of
91 decades to centuries, however, anthropogenic impacts would shift natural DOM to forms of low-molecular weight, enhanced
92 redox state with potentially increased lability, or increased aromaticity due to warmer climate and altered hydrology
93 (Stanley et al., 2012; Xenopoulos et al., 2021).

94 In this study, we evaluated how geomorphologic controls (i.e., mean catchment slope and mean drainage elevation) and
95 anthropogenic impacts (i.e., land use patterns) affect the DOC dynamics and DOM characteristics in three subtropical
96 catchments encompassing numerous small to medium mountainous rivers in southwest China. Our prior observations from
97 these catchments showed that particulate organic carbon (POC) and dissolved inorganic carbon (DIC) dynamics were highly
98 affected by in-stream photosynthesis, as evidenced by stable carbon isotope and radioactive carbon isotope of POC and DIC
99 (Chen et al., 2021). We hypothesize that catchments with a higher proportion of agricultural and urban land use, gentler
100 catchment slope, and lower elevation would exhibit higher riverine DOC concentrations and more autochthonous microbial
101 humic-like DOM than steeper catchments at high elevations with fewer influences by agricultural and urban land uses.
102 Relationships of DOC concentrations, stable isotopic values of DOC, DOM quality assessed through optical metric, nutrient
103 concentrations, and land use patterns versus geomorphologic characteristics (i.e., mean catchment slope and mean drainage
104 elevation) were examined. We also examined relationships between geomorphologic characteristics and radiocarbon for nine
105 sampling sites in the Yinjiang River. This study allows us to gain a deeper insight into the geomorphologic controls and
106 anthropogenic impacts on DOC dynamics and DOM quality in the subtropical, anthropogenically influenced mountainous
107 rivers.

108 **2 Materials and Methods**

109 **2.1 Study area**

110 Yinjiang River (Y), Shiqian River (S), and Yuqing River (Q) are tributaries of the Wujiang River (Fig. 1a), the largest
111 tributary on the south bank of the upper Changjiang River. The drainage area is 1231, 2101, and 1561 km² for the Yinjiang,
112 Shiqian, and Yuqing rivers, respectively. Data on land use types and air temperature in 2015, as well as a 90 m digital
113 elevation model (Shuttle Radar Topography Mission, SRTM) were obtained from the Resource and Environment Data Cloud
114 Platform of the Chinese Academy of Sciences (<http://www.resdc.cn/>). The SOC content in the surface layer (0–5 cm) was
115 collected from the SoilGrids1km database (a global soil information system at 1 km resolution) (Hengl et al., 2014).
116 Information on dams was retrieved from Wang et al. (2022), and their location was identified by Google Earth. Furthermore,
117 the distance from the river mouth (i.e., the Yinjiang, Shiqian, and Yuqing rivers) to the sampling sites was also estimated
118 using Google Earth. We further delineated the sub-catchments, which constitute the contributing area upstream of sampling
119 sites, by spatial analyst tools of ArcGIS (version 10.2). The mean catchment slope (degrees; 3D analysis tools) and elevation
120 for sub-catchments were extracted from the digital elevation model using ArcGIS. Annual air temperature (T_{air}), catchment
121 slope, topsoil SOC, and proportion of urban and agricultural land use for these sub-catchments were also determined using
122 ArcGIS. The mean drainage elevation of these three catchments ranges from 340 m to 2424 m, with the lowest and highest
123 elevations both reported in the Yinjiang River catchment, showing the greatest change in relief (Figs. 1a and S1a). The



124

125 **Figure 1.** Map of the study area. (a) Overview of the sampling sites and elevation characteristics in the three study catchments, including
 126 the Yinjiang, Shiqian, and Yuqing catchments, (b) correlation between mean catchment slope and the distance from the river mouth (i.e.,
 127 the Yinjiang, Shiqian, and Yuqing rivers) to the sampling site, and (c) spatial variation in land-use patterns.

128

129

130

131

132

133

134

135

136

137

138

139

140

topsoil SOC exhibited a spatial distribution that resembled elevation, with regions with higher elevation displaying higher SOC contents (Fig. S2). Similar to elevation, the Yinjiang River catchment has a greater variation in mean catchment slope (from 14.3° to 25.5°), while the Shiqian and Yuqing river catchments have a mean catchment slope of approximately 20°, except the segment above site S8 (13.9°; Figs. 1b and S1b). Carbonate rock is widely distributed in the three catchments, accounting for a large proportion of the exposed strata (Han and Liu, 2004). The remaining areas are mainly covered by elastic rocks, igneous rocks, and low-grade metamorphic rocks. Forest, agriculture, and urban areas are the three dominant land uses in these studied catchments (Fig. 1c). Forest is generally distributed in high-elevation regions, while urban and agricultural land uses are mainly located in low-elevation regions. The proportion of urban and agricultural land uses in the Yuqing River catchment varies from 17.3% to 23.1% (Figs. 1c and S1c). This catchment has a higher % urban/agriculture land use than other studied catchments and less variability in land use compared to the Yinjiang and Shiqian river catchments (from 4.5% to 46.5% and from 9.6% to 41.3%, respectively). There are three mountainous agricultural counties (i.e., Yinjiang, Shiqian, and Yuqing; Fig. 1a) in this study area, where crops are mainly C4 (e.g., corn and sorghum) and C3 (e.g., rice, wheat, and potato) plants. Dams and reservoirs are widely distributed in the three catchments, and these dams are

141 primarily used for agricultural irrigation and power generation (Fig. 1a). This study area is highly affected by
142 monsoon-influenced humid subtropical climate with April to October being the rainy season, and the average annual
143 precipitation, runoff, and discharge are 1100 mm, 1004 mm/yr and 14.4 m³/s, respectively, in the Yinjiang River catchment.
144 Further details on the regional setting of the study area and the sources and methods for catchment characteristics delineation
145 are provided in our previous study (Chen et al., 2021).

146 **2.2 Field sampling**

147 Surface water samples (n = 28) along the mainstem and major tributaries of the Yinjiang River, Shiqian River, and Yuqing
148 River and spring water samples (n = 4) were collected in September 2018 (Fig. 1a). During the sampling period, two water
149 samples (sites Y12 and Y15) were significantly affected by rainfall events, and an additional sample was collected at site
150 Y12 before the rainfall event as it is close to the hydrological station. Unless stated otherwise, the data used in this study
151 from site Y12 are based on the sample collected after rainfall events due to the availability of carbon isotopes. Electrical
152 conductivity (EC) and dissolved oxygen (DO) were measured by a multi-parameter water quality probe (WTW, pH
153 3630/Cond 3630, Germany) in the field. For the analysis of ion concentrations, total phosphorus (TP), ammonium (NH₄⁺-N),
154 and total nitrogen (TN), water samples were filtered through 0.45 μm cellulose acetate membranes. Water samples for the
155 concentrations and isotopes of DOC and DOM absorbance and fluorescence were filtered through pre-combusted glass fibre
156 filters (Whatman, 0.7 μm). The filtered water was stored in a Milli-Q water and sampling water pre-washed brand-new
157 low-density polyethylene container at low temperature (4°C) in the dark within one week before optical properties analysis
158 and acidified by phosphoric acid to pH = 2 for DOC analysis. Water samples were also filtered for determining DIC (through
159 0.45 μm cellulose acetate membranes) through titration with hydrochloric acid and analyzing POC using retained suspended
160 particles on the filter membranes. The water samples filtered through 0.22 μm cellulose-acetate filter membranes were used
161 to determine water isotopes (δ¹⁸O and δD). Detailed information on sampling methods was provided in Chen et al. (2021)
162 and Zhong et al. (2020).

163 **2.3 Laboratory analysis**

164 The main cations (K⁺, Na⁺, Ca²⁺, and Mg²⁺) were measured by inductively coupled plasma emission spectrometer
165 (ICP-OES), and the main anions (Cl⁻, SO₄²⁻, and NO₃⁻) were measured by ion chromatography (Thermo Aquion; Chen et al.,
166 2020). The normalized inorganic charge balance is within 5%, indicating the accuracy of the measured data. The
167 concentrations of NH₄⁺-N were analyzed using an automatic flow analyzer (Skalar Sans Plus Systems), and the relative
168 deviations of the results of NH₄⁺-N were less than 5%. DOC concentrations were determined with a total organic carbon
169 analyser (OI Analytical, Aurora 1030W, USA) with duplicates (±1.5%, analytical error) and a detection limit at 0.01 mg L⁻¹.
170 Water isotopes were measured by a Liquid Water Isotope Analyzer (Picarro L2140-i, USA) with measurement precisions at ±

171 0.3 ‰ for $\delta^{18}\text{O}$. The above analyses were carried out at the Institute of Surface Earth System Science, Tianjin University.

172 For the determination of stable carbon isotope and radiocarbon isotope of DOC ($\delta^{13}\text{C}_{\text{DOC}}$ and $\Delta^{14}\text{C}_{\text{DOC}}$), water samples
173 were first concentrated using a rotary evaporation and then oxidized through the wet oxidation method (Leonard et al., 2013).
174 In this study, nine water samples collected from the Yinjiang River were selected for $\Delta^{14}\text{C}_{\text{DOC}}$ analysis as the Yinjiang River
175 catchment has the greatest change in geomorphologic characteristics (i.e., elevation and catchment slope) and the highest
176 proportion of agricultural and urban land uses among the three catchments. The generated CO_2 was purified in a vacuum
177 system for $\delta^{13}\text{C}_{\text{DOC}}$ and $\Delta^{14}\text{C}_{\text{DOC}}$ analyses, respectively. $\delta^{13}\text{C}_{\text{DOC}}$ was directly determined by the MAT 253 mass spectrometer
178 with an analysis accuracy of ± 0.1 ‰. For $\Delta^{14}\text{C}_{\text{DOC}}$ analysis, the purified CO_2 was transformed into graphite following the
179 same method of $\Delta^{14}\text{C}_{\text{POC}}$ analysis (Chen et al., 2021) and measured by an accelerator mass spectrometry (AMS) system
180 within 24 hours with an analytical error of ± 3 ‰ (Dong et al., 2018).

181 Optical analyses on DOM were conducted on river samples. DOM absorbance of river water samples was measured from
182 250 to 750 nm at 1 nm intervals using a UV (ultraviolet)-visible spectrophotometer (UV-2700, Shimadzu) with a 1 cm quartz
183 cuvette. The UV-visible spectrophotometer was blanked with Milli-Q water prior to data collection. Decadic absorbance
184 values were used to calculate absorption coefficients as below (Poulin et al., 2014):

$$185 \quad a_{254} = \text{Abs}_{254}/L, \quad (1)$$

186 Where, a_{254} is the absorption coefficient (m^{-1}), Abs_{254} is the absorbance at 254 nm, and L represents the path length (m).
187 Specific UV absorbance at 254 nm (SUVA_{254} ; reported in units of $\text{L mg C}^{-1} \text{m}^{-1}$) was determined according to Weishaar et al.
188 (2003; Table 1):

$$189 \quad \text{SUVA}_{254} = a_{254}/\text{DOC}. \quad (2)$$

190 DOM fluorescence was determined with a fluorescence spectrophotometer (F-7000, Hitachi, Japan) to quantify
191 humic-like, fulvic-like, and protein-like fluorescences (Fellman et al., 2010). The fate of humic-like fluorescences may be
192 self-assembly particles or be adsorbed onto minerals, while protein-like fluorescences are tightly associated with biological
193 processes, and biodegraded into inorganic matter (Fellman et al., 2010; He et al., 2016). The excitation wavelengths ranged
194 from 220 to 400 nm at 5 nm increments, and the emission wavelength from 280 to 500 nm at 2 nm increments. Blanks were
195 measured daily with the same settings to correct excitation-emission matrices (EEMs). Parallel factor analysis (PARAFAC)
196 was performed using the N-way toolbox in Matlab (MathWorks, USA) to determine peaks (Andersson and Bro, 2000;
197 Mostofa et al., 2019; Stedmon and Bro, 2008). Detailed procedures and criteria for applying and validating the PARAFAC
198 model are available in Yi et al. (2021). Identified PARAFAC model components were further compared with relevant
199 published and reported fluorophores in the OpenFluor database (Table 1; Murphy et al., 2014). Several common indices of
200 DOM composition were determined from EEMs, including fluorescence index (FI; McKnight et al., 2001), humification
201 index (HIX; Ohno, 2002), and freshness index (β/α ; Parlanti et al., 2000; Table 2).

202 **Table 1.** Description of the three components identified by PARAFAC and comparison with previous studies from the
 203 OpenFluor database with a minimum similarity score of 0.95 (Murphy et al., 2014).

Component	$E_{X_{max}}$ (nm)	$E_{m_{max}}$ (nm)	Description and likely structure	Number of matches in Openfluor	Previous studies
C1	295	402	Similar to traditionally defined peak M, marine humic-like components, are products from microbial processes or autochthonous production.	6	C6 (Walker et al., 2009); C4 (Kim et al., 2022); C4 (Li et al., 2016)
C2	275	338	Protein-like (Tryptophan-like) components, commonly found in anthropogenically affected rivers, are associated with recent biological production and breakdown products of lignin.	30	C3 (DeFrancesco and Guéguen, 2021); C7 (Lambert et al., 2017); C2 (Du et al., 2019)
C3	325	440	Traditional fulvic-like peaks A and C, humic-like and terrestrial delivered OM, autochthonous, or microbial source.	70	C1 (Amaral et al., 2016); C1 (Ryan et al., 2022); C1 (Shutova et al., 2014)

204

205 **2.4. Statistical analysis**

206 Normality of the data was first examined by a Shapiro-Wilk test using SPSS 26. Normally distributed data were analyzed by
 207 one-way ANOVA with Tukey's post-test for multiple comparisons. Nonparametric data with three or more comparisons were
 208 made by Kruskal–Wallis test followed by Holm's Stepdown Bonferroni correction. The Mann–Whitney U test was used for
 209 comparison of distributions between two groups. The correlations among DOC concentrations, DOM properties, carbon
 210 isotopes, ion concentrations, and catchment characteristics (i.e., mean catchment slope, the proportion of different land uses,
 211 mean annual air temperature, and mean drainage elevation) were computed by Pearson's correlation coefficients (R) by
 212 OriginPro 2021 (student version). Values are presented as the mean \pm standard deviation. All statistical tests were performed
 213 at a 0.05 significance level. In addition, all the statistical analyses were performed again after data from site Y12 were
 214 removed to test the possible skew of findings, as the sample was significantly affected by rainfall events. If not mentioned
 215 otherwise, the results from site Y12 did not skew the findings at the significance level of 0.05.

216 We performed a stepwise multiple linear regression (MLR) modeling to identify significant environmental factors of
 217 DOC concentrations and DOM properties using SPSS 26. All environmental factors were included in the models except for
 218 SOC because we aim to examine the impacts of human activities and geomorphology rather than the direct influence of SOC
 219 on DOC concentrations and DOM properties. The objective model with the highest adjusted R^2 value was used to infer the
 220 DOC concentrations and DOM properties. In addition to the MLR and Pearson correlation analyses to explore the

relationships between environmental factors and DOC, we further performed the partial least squares path model (PLS-PM) to infer direct and indirect effects of multiple factors (e.g., geomorphologic and anthropogenic impacts) on DOC concentrations. The PLS-PM analysis was performed using the R package “plsmpm” (Sanchez, 2013). Because PLS-PM offers the advantage of not imposing any distributional assumptions on the data, which enhances its broad applicability (Sanchez, 2013), and allows for the exploration of complex cause-effect relationships involving latent variables, it is a suitable technique for multivariate analyses. Each latent variable consists of one or more manifest variables (e.g., geomorphology, including elevation and slope). The environmental factors used in the model were categorized into seven latent variables, including geomorphology (elevation and slope), anthropogenic activities (e.g., urban and agricultural land uses and anthropogenically derived Cl^- ($\text{Cl}^-_{\text{anthro}}$, calculated as the total Cl^- concentration minus atmospheric contributed Cl^- concentration, which is the lowest Cl^- concentration at site Y5 in the Yinjiang River; Gaillardet et al., 1997; Meybeck, 1983)), climate (T_{air}), SOC (SOC content), water chemistry (pH), POC (POC concentrations) and nutrient (NH_4^+ -N and TN). The environmental factors and their manifest variables included in the model were the most critical variables identified based on the Pearson correlation results. These variables were selected after reducing the full models (initial models with more variables) to meet the requirements of the PLS-PM analysis (Du et al., 2023; Sanchez, 2013; Tian et al., 2019). In addition, the structure of the model was simplified to focus on the major effect of environmental factors on DOC concentrations rather

Table 2. DOM optical parameters were used in this study.

Index Name	Calculation	Description	Reference
SUVA ₂₅₄	SUVA ₂₅₄ = $a_{254}/\text{DOC concentration}$. a_{254} is the decadic UV absorbance at 254 nm.	An indicator for the degree of aromaticity. It is positively correlated with aromaticity.	Weishaar et al. (2003)
Fluorescence index (FI)	FI = $\text{Em}_{450}/\text{Em}_{500}$, at Ex 370 nm.	A proxy for DOM source. Higher values (~1.9) were associated with microbial sources, and lower values (~1.4) correlated with terrestrial sources.	McKnight et al. (2001)
Humification index (HIX)	HIX = $\frac{\sum 435-480}{\sum 300-345 + \sum 435-480}$, at Ex 254 nm.	Indicator of humification status of DOM. Higher HIX values indicate an increasing degree of humification.	Ohno (2002)
Freshness index (β/α)	$\beta/\alpha = \text{Em}_{380}(\beta) / \text{the Em intensity maximum between 420 and 435 nm at Ex 310 nm}(\alpha)$.	Higher β/α values are commonly associated with the increasing contribution of recently microbially produced DOM.	Parlanti et al. (2000)

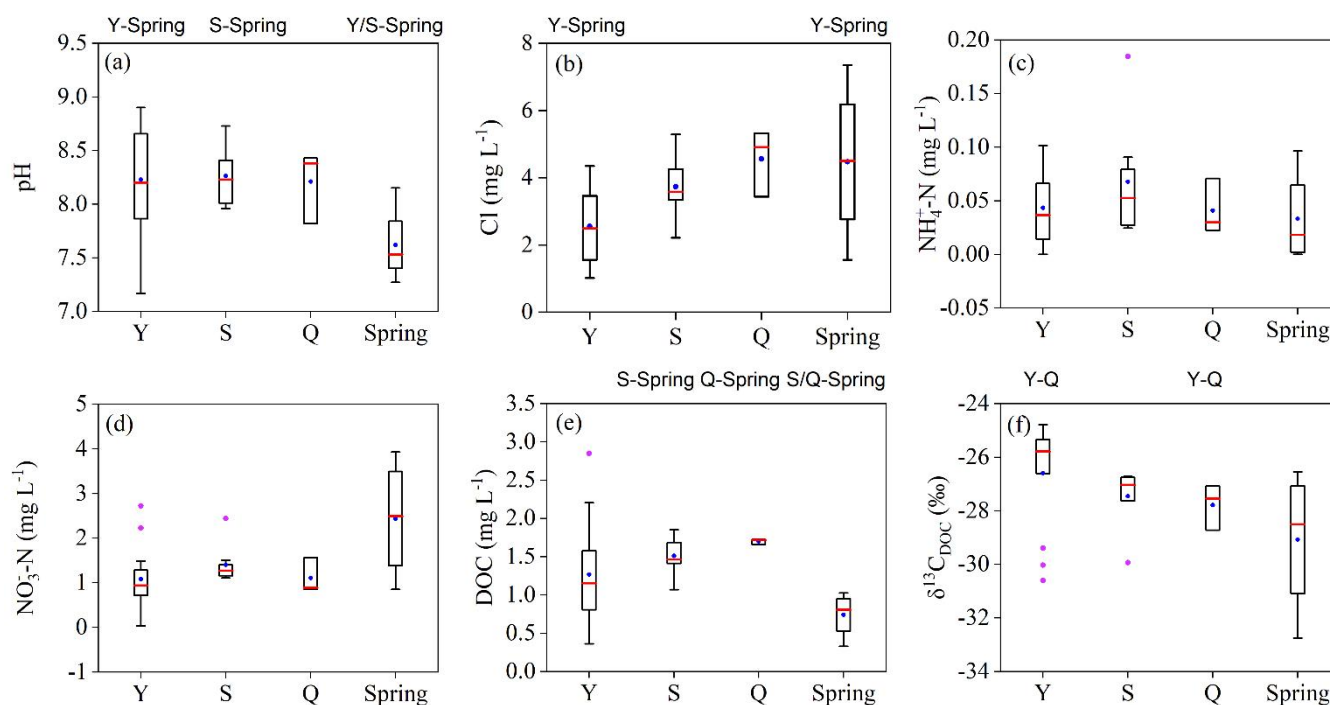
238 than to explore the effects on other factors (e.g., the geomorphologic controls on POC were ignored). The significance of
 239 the path coefficients was determined through a nonparametric bootstrap resampling of 1000 times.

240 3 Results

241 3.1 Spatial variations in water chemistry, DOC concentrations, and isotopes of DOC

242 Both river water and spring water were mildly alkaline with pH varying from 7.2 to 8.9, and the pH in the Yinjiang and
 243 Shiqian rivers was higher than that in the spring water (Fig. 2a). The Cl⁻ concentration showed an increasing trend in the
 244 Yinjiang, Shiqian, and Yuqing rivers, with an average of 2.56 ± 1.03 mg L⁻¹, 3.76 ± 0.83 mg L⁻¹, and 4.55 ± 0.81 mg L⁻¹,
 245 respectively (Fig. 2b). In addition, the Cl⁻ concentration in the spring water (4.48 ± 2.08 mg L⁻¹) was significantly higher
 246 than that in the Yinjiang River ($p < 0.05$; Fig. 2b). Within the rivers and springs, the water displayed similar NH₄⁺-N
 247 concentrations with the mean value at 0.04 ± 0.03 mg L⁻¹, 0.07 ± 0.05 mg L⁻¹, 0.04 ± 0.03 mg L⁻¹, and 0.03 ± 0.04 mg L⁻¹ in
 248 the Yinjiang, Shiqian, Yuqing rivers, and spring water (Fig. 2c). In springs, the average NO₃⁻-N concentration was $1.93 \pm$
 249 0.93 mg L⁻¹, higher than the average in the three rivers (1.15 ± 0.36 mg L⁻¹), though there were no significant differences for
 250 the overall NO₃⁻-N concentration between the rivers and springs ($p > 0.05$; Figs. 2d).

251



252 **Figure 2.** Spatial variations in water chemistry in the Yinjiang (Y), Shiqian (S), and Yuqing (Q) rivers and springs. (a) pH, (b) Cl⁻, (c)
 253 NH₄⁺-N, (d) NO₃⁻-N, (e) DOC, and (f) δ¹³C_{DOC}. In each box plot, the end of the box represents the 25th and 75th percentiles, the blue solid
 254 dot represents the mean, the horizontal line inside the box represents the median, and the whiskers represent 1.5 times the upper and lower
 255 interquartile ranges (IQR). The magenta solid dot represents the outlier (data points outside of the 1.5 interquartile ranges). Letters above
 256 the boxes represent significant differences between the grouping of river and/or spring water based on statistical analyses at the
 257 significance level of 0.05 (e.g., Y-Spring above panel (b) indicates that the Cl⁻ in river water of the Yinjiang River was significantly
 258 different from that in the spring water).
 259

260 DOC concentrations in the three study rivers varied from 0.36 to 2.85 mg L⁻¹ with the highest mean concentration in the
 261 Yuqing River (1.70 ± 0.04 mg L⁻¹; Fig. 2e), followed by the Shiqian River (1.51 ± 0.22 mg L⁻¹) and the Yinjiang River (1.27
 262 ± 0.66 mg L⁻¹). The DOC concentrations in spring water were significantly lower than those in the surface water of the
 263 Shiqian and Yuqing rivers ($p < 0.05$; Fig. 2e), and the average DOC concentration in spring water (0.74 ± 0.30 mg L⁻¹) was
 264 also lower than the average DOC concentration in the Yinjiang River, indicating there must be other sources of DOC besides
 265 groundwater.

266 For $\delta^{13}\text{C}_{\text{DOC}}$, although the average $\delta^{13}\text{C}_{\text{DOC}}$ values showed a decreasing trend in the Yinjiang River, Shiqian River, Yuqing
 267 River, and springs, averaging at $-26.6 \pm 1.8 \text{ ‰}$, $-27.5 \pm 1.1 \text{ ‰}$, $-27.8 \pm 0.9 \text{ ‰}$, and $-29.1 \pm 2.7 \text{ ‰}$, respectively, there were no
 268 statistically significant differences on the overall $\delta^{13}\text{C}_{\text{DOC}}$ values between the three rivers and springs ($p > 0.05$; Fig. 2f). The
 269 $\Delta^{14}\text{C}_{\text{DOC}}$ of the Yinjiang River varied widely from -109 ‰ to 33 ‰ with an average of $-54.7 \pm 39.9 \text{ ‰}$ (Table 3). The
 270 radiocarbon ages of the DOC ranged from 928 years BP (i.e., before present) to present, and the youngest $\Delta^{14}\text{C}_{\text{DOC}}$ (33.3 ‰)
 271 was found at site Y12.

272 **Table 3.** $\Delta^{14}\text{C}_{\text{DOC}}$ and age of DOC in the Yinjiang River.

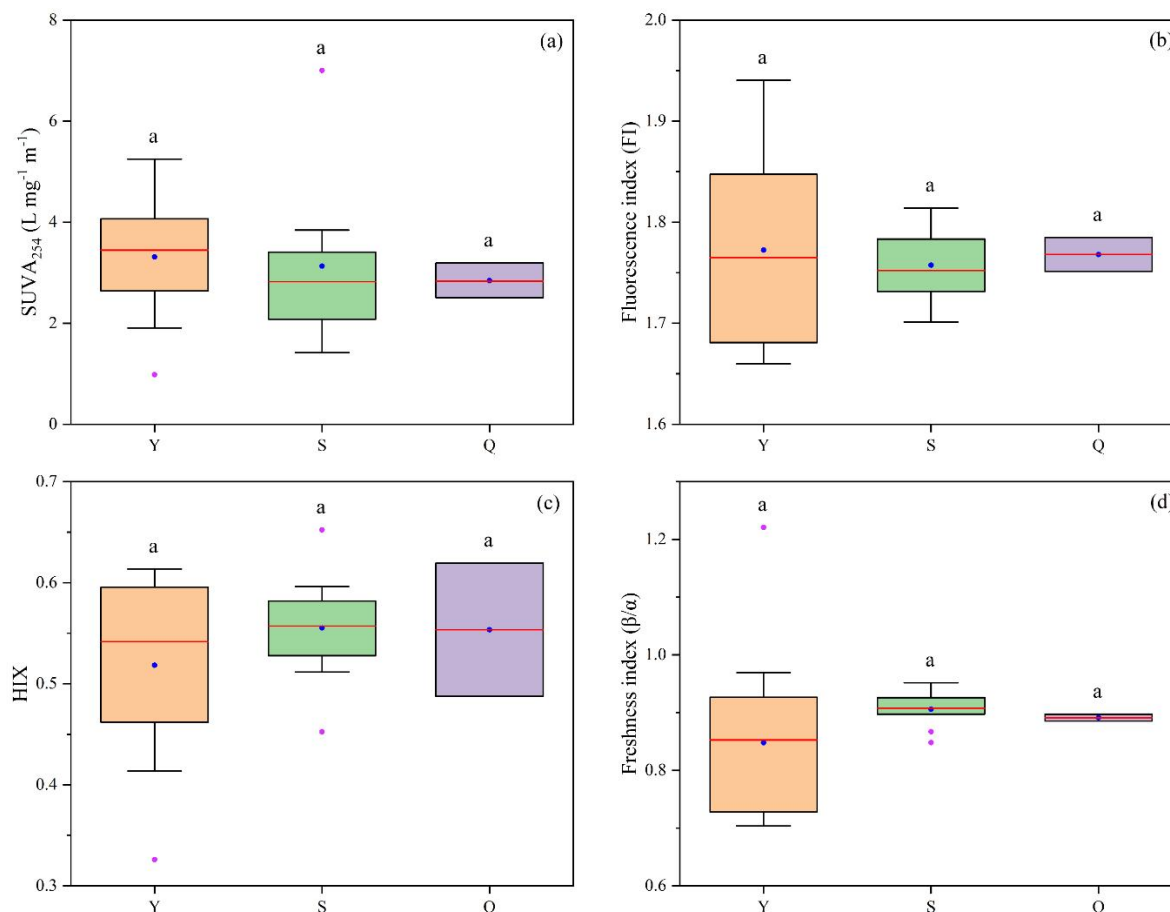
River	Samples	$\Delta^{14}\text{C}_{\text{DOC}}$ (‰)	DOC-Age (yr BP)	SD of DOC-Age (yr BP)
Yinjiang River	Y1	-92	774	25
	Y2	-74	616	23
	Y3	-52	430	27
	Y5	-40	326	27
	Y9	-59	491	27
	Y11	-51	417	27
	Y12	33	Modern	28
	Y13	-49	401	24
	Y14	-109	928	28

273 3.2. Riverine DOM optical properties

274 Two humic-like fluorescence components (C1 and C3) and one protein-like fluorescence component (C2) were
 275 identified by the PARAFAC model in these three rivers (Fig. S3; Table 1). Component C1 is similar to traditionally
 276 defined peak M and sourced from microbial processes or autochthonous production (Kim et al., 2022; Li et al., 2016;
 277 Walker et al., 2009). Component C2 was previously related to recent biological production (DeFrancesco and Guéguen,
 278 2021; Du et al., 2019; Lambert et al., 2017). C3 was the most widely found component in previous research among three

279 fluorescence components and was identified as traditional fulvic-like peaks A and C, representing terrestrial delivered
 280 OM or autochthonous microbial sourced OM (Amaral et al., 2016; Ryan et al., 2022; Shutova et al., 2014). Although C1
 281 and C2 varied more widely in the Yinjiang River compared with the Shiqian and Yuqing rivers, the two fluorescence
 282 components did not show a statistical difference among the three rivers ($p > 0.05$; Figs. S3a and b). However, a greater
 283 proportion of C3 was found in the Shiqian River, exhibiting a distinctive signature compared with the Yinjiang River
 284 (Fig. S3c). The proportion of C3 did not show any significant differences between the Yuqing River and the other two
 285 rivers (the Yinjiang and Shiqian rivers).

286 The average $SUVA_{254}$ were 3.3 ± 1.1 , 3.1 ± 1.8 , and 2.8 ± 0.3 $L\ mg^{-1}\ m^{-1}$ in the Yinjiang, Shiqian, and Yuqing rivers,
 287 respectively, without significant spatial differences across the three rivers ($p > 0.05$; Fig. 3a). For the fluorescence
 288 indexes, the overall fluorescence property did not vary significantly among the three rivers ($p > 0.05$; Figs. 3b, c, and d).
 289 FI varied in a narrow range compared with β/α and HIX. FI of DOM ranged from 1.66 to 1.94, averaging 1.78 (Fig. 3b),
 290 indicating a mixture of DOM of terrestrial and microbial origins. In comparison, β/α varied from 0.70 to 1.22 (Fig. 3d)
 291 and HIX varied from 0.33 to 0.65 (Fig. 3c), with greater variability among the three rivers.

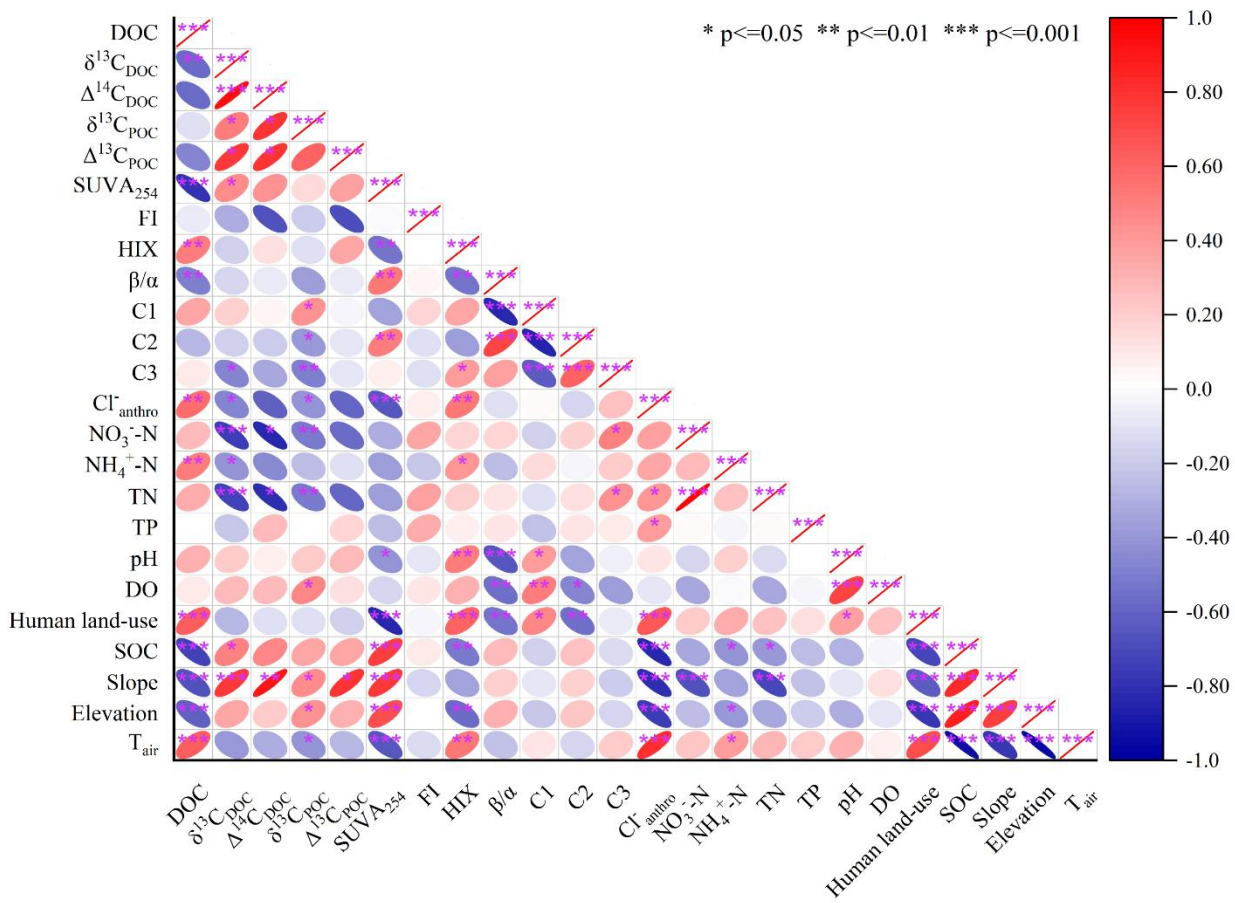


292
 293 **Figure 3** Spatial variations in DOM property in the Yinjiang (Y), Shiqian (S), and Yuqing (Q) catchments. (a) $SUVA_{254}$, (b) fluorescence
 294 index (FI), (c) HIX, and (d) freshness index (β/α). In each box plot, the end of the box represents the 25th and 75th percentiles, the blue
 295 solid dot represents the average, the horizontal red line represents the median, and the whiskers represent 1.5 IQR. The magenta solid dot
 296 represents the outlier, which is outside of the 1.5 interquartile range. Different lowercase letters above the boxes denote significant
 297 differences across rivers based on statistical analysis with $p < 0.05$.

298 3.3. Factors influencing DOC concentrations, isotopes of DOC, and DOM optical properties

299 Significant pairwise interdependencies between DOC and catchment characteristics were identified in the three study rivers
300 (Fig. 4). There is a strong negative correlation between DOC and SOC, as well as average catchment slope ($p < 0.01$; Fig.
301 4a). Conversely, DOC displayed a positive correlation with the proportion of urban and agricultural land uses ($p < 0.01$),
302 Cl_{anthro} ($p < 0.05$), and NH_4^+-N ($p < 0.001$). Stepwise MLR models revealed that topsoil SOC and POC were the most
303 effective predictors for explaining the spatial variation in DOC concentrations (Table 4), while catchment slope and NH_4^+-N
304 exhibited the highest explanatory power for DOC concentrations when SOC was excluded from the models. Unlike DOC, a
305 significant positive correlation with mean catchment slope was found for $\delta^{13}C_{\text{DOC}}$ ($p < 0.001$; Fig. 4). In addition, there was a
306 significant negative correlation between $\delta^{13}C_{\text{DOC}}$ and $NO_3^- - N$ ($p < 0.001$). Moreover, $\delta^{13}C_{\text{DOC}}$ was negatively correlated with
307 DOC concentrations ($p < 0.01$), but positively correlated with $\delta^{13}C_{\text{POC}}$ in these three rivers ($p < 0.05$). Similar to $\delta^{13}C_{\text{DOC}}$,
308 $\Delta^{14}C_{\text{DOC}}$ was positively related to mean catchment slope ($p < 0.01$) and $\Delta^{14}C_{\text{POC}}$ ($p < 0.01$). Additionally, there was a positive
309 correlation between $\Delta^{14}C_{\text{POC}}$ and catchment slope ($p < 0.001$), and no significant correlations were detected between $\Delta^{14}C_{\text{POC}}$
310 and the proportion of urban and agricultural land uses or ions that reflect human disturbances (e.g., Cl_{anthro} , NH_4^+-N , and
311 $NO_3^- - N$; $p > 0.05$; Fig. 4).

312 SUVA₂₅₄ showed an increasing trend with increasing mean catchment slope ($p < 0.001$; Fig. 4). Furthermore, there was a
313 significant negative correlation between SUVA₂₅₄ and the proportion of urban and agricultural land uses ($p < 0.001$; Fig. 4).
314 This is consistent with the constructed stepwise MLR models that urban and agricultural land uses and catchment slope were
315 the best predictors of SUVA₂₅₄ (Table 4). Although no significant correlation was observed between the fluorescence indexes
316 and catchment slope, they (except for FI) were found to be closely related to land use patterns (Fig. 4). For example, HIX
317 had a positive correlation with urban and agricultural land uses ($p < 0.001$; Fig. 7e), while β/α had a negative correlation with
318 urban and agricultural land uses ($p < 0.01$; Fig. 4) and water pH ($p < 0.001$; Fig. 4). In addition, the fluorescence components
319 did not exhibit significant variations with changing catchment slope ($p > 0.05$; Fig. S4), but the percentage of C1 and C2
320 were positively ($p < 0.05$; Fig. 7b) or negatively ($p < 0.01$; Fig. 7c) related to the proportion of urban and agricultural land
321 uses. Urban and agricultural land uses were also identified as predictors for DOM optical indexes (i.e., HIX; Table 4) and
322 fluorescent components (i.e., C1 and C2). However, unlike C1 and C2, C3 was not significantly correlated with urban and
323 agricultural land uses ($p > 0.05$; Fig. 4), but its variation can be partially explained by $NO_3^- - N$ concentrations and POC
324 (Table 4).



325

326 **Figure 4.** Correlation plot of the selected water chemistry and catchment characteristics. The colors represent the degree of pairwise
 327 correlation regarding Pearson's correlation coefficient. $\delta^{13}\text{C}_{\text{DOC}}$ and $\Delta^{14}\text{C}_{\text{DOC}}$ at site Y12 were excluded from the analysis as the sample was
 328 collected after a rainfall event. In addition, SUVA_{254} at site S3 was excluded from the analysis as the sample was strongly influenced by
 329 road construction, which was evidenced by high POC and TSM concentration (Chen et al., 2021). Human land use denotes the proportion
 330 of urban and agricultural land uses. Elevation and T_{air} represent mean drainage elevation and annual air temperature, respectively.

331 **3.4. Direct and indirect effects of environmental factors on DOC concentrations**

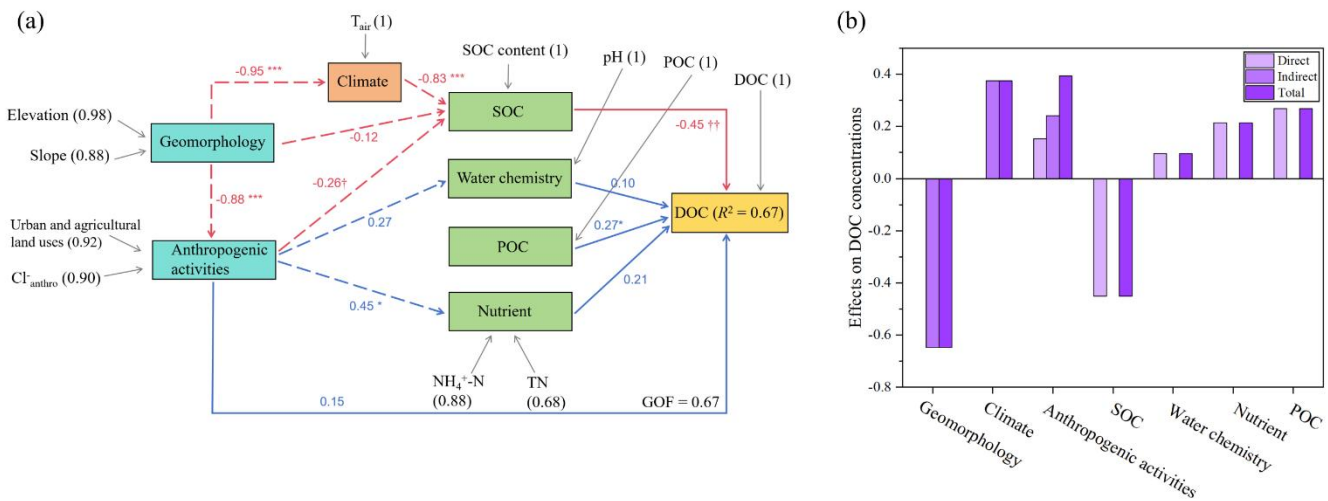
332 The PLS-PM analysis showed that 67% of the variance in DOC concentrations could be explained by our constructed seven
 333 environmental factors ($R^2 = 0.67$, Fig. 6a). The total effect on DOC concentrations is strongest from geomorphology (-0.65),
 334 followed by SOC (-0.45), anthropogenic activities (0.39), climate (0.38), POC (0.27), nutrient (0.21), and water chemistry
 335 (0.10) (Fig. 6b). The results indicated that geomorphology was the most significant factor in controlling DOC concentrations,
 336 primarily through indirect regulation on SOC content, which was directly influenced by annual catchment temperature and
 337 anthropogenic activities (Figs. 6a and b). In comparison, anthropogenic activities not only indirectly regulated riverine DOC
 338 concentrations through SOC, but also had a significant indirect impact through the regulation of nutrient levels. Similar to
 339 DOC concentrations, geomorphology (-0.53) exhibited the most pronounced effects on fluorescent components (Fig. S4).
 340 However, anthropogenic activities (0.49) demonstrated a comparable effect on fluorescent components, primarily through a
 341 direct pathway (0.37; Fig. S4b). Anthropogenic activities (-0.84) were the strongest driver for DOM optical parameters,
 342 although geomorphology (0.59) played a significant role in indirectly influencing DOM optical parameters (Fig. S5).

343 **Table 4.** Multiple stepwise linear regression models of catchment attributes and water chemistry on DOC concentrations and
 344 DOM properties.

Dependent variables	Predictors	Model equation	<i>n</i>	Adj <i>R</i> ²	Significance level
DOC ^a	slope, NH ₄ ⁺ -N	= -0.109*slope + 4.295*NH ₄ ⁺ -N + 3.375	28	0.50	<i>p</i> < 0.001
DOC	SOC, POC	= -0.006*SOC + 0.384*POC + 4.145	28	0.59	<i>p</i> < 0.001
SUVA ₂₅₄	urban and agricultural land use, slope	= -5.461*urban and agricultural land use + 0.145*slope + 1.318	26	0.77	<i>p</i> < 0.001
HIX	urban and agricultural land use	= 0.433*urban and agricultural land use + 0.438	27	0.34	<i>p</i> < 0.001
FI		No variables were entered into the equation.	27		
β/α	pH	= -0.195*pH + 2.476	27	0.41	<i>p</i> < 0.001
C1	DO, TP, urban and agricultural land use	= 7.713*DO - 220.846*TP + 90.905*urban and agricultural land use - 36.005	27	0.46	<i>p</i> < 0.001
C2	urban and agricultural land use, DO	= -48.748*urban and agricultural land use - 2.515*DO + 58.255	27	0.36	<i>p</i> = 0.002
C3	NO ₃ ⁻ -N, POC	= 4.181*NO ₃ ⁻ -N + 3.738*POC + 3.826	27	0.34	<i>p</i> = 0.003

345 ^a SOC was not included as predictors in this model to examine the impacts of human activities and geomorphology, rather than the direct
 346 influence of SOC on DOC concentrations.

347



348

349 **Figure 6.** The most parsimonious PLS-PM model shows the direct and indirect effects of geomorphology and anthropogenic activities on
 350 DOC concentrations. (a) Path coefficients are shown as arrows with blue and red to represent positive and negative effects, respectively.
 351 The solid and dotted lines indicate the direct and indirect influence pathways of environmental drivers on DOC concentrations,
 352 respectively. The indicators (e.g., TN) of latent variables (e.g., nutrient) are shown at the beginning of the grey arrows. The numbers in the
 353 parentheses are the loading scores. GOF denotes the goodness of fit of the entire model. *R*² indicates the amount of variance in DOC
 354 concentrations explained by its independent latent variables. The standardized path coefficients that are significantly different from zero
 355 are indicated by **p* < 0.05, ***p* < 0.01, ****p* < 0.001, †*p* = 0.06, ††*p* = 0.07. (b) Standardized direct and indirect mean effects of
 356 environmental drivers on DOC concentrations derived from the PLS-PM analysis.

357 4 Discussion

358 4.1 Geomorphologic controls on DOC export

359 Catchment slope, which is often closely associated with catchment elevation (Fig. 4), is an important predictor of DOC
360 concentrations because catchment slope is a key factor in affecting flow velocity and thus water retention time (Harms et al.,
361 2016; Mzobe et al., 2020). The negative relationship between DOC and SOC (Fig. 4 and Table 4) and the positive correlation
362 between slope and $\Delta^{14}\text{C}_{\text{POC}}$ or $\Delta^{14}\text{C}_{\text{DOC}}$ is consistent with previous findings that a shorter water retention time in high relief
363 regions can reduce DOC export from SOC stocks and mobilize organic carbon with younger ages (Catalán et al., 2016). The
364 decreasing organic carbon export in catchments with higher slopes partially explains why high-relief regions exhibit lower
365 riverine DOC concentrations despite having a higher SOC content. Compared with high-relief regions, low-relief regions
366 would discharge more aged organic carbon into rivers when relatively ^{14}C -depleted DIC and CO_2 (aq) derived from
367 carbonate weathering are incorporated into primary production in low-relief regions, as also evidenced by the positive
368 relationship between slope and $\Delta^{14}\text{C}_{\text{POC}}$ (Fig. 4). Furthermore, the aged riverine DOC has also been attributed to the input of
369 deeper, older soil organic matter through deeper flow paths (Barnes et al., 2018; Masiello and Druffel, 2001). This aged DOC,
370 discharged through deeper water flow paths, may have also served as an important source of DOC in low relief regions of
371 this study. The correlation of SUVA_{254} with the mean catchment slope suggests that steeper catchments tend to export DOC
372 with more aromaticity (Fig. 4 and Table 4), indicating the geomorphologic effects on DOM characteristics. Previous research
373 has reported that the aromatic content of DOM tends to decline if DOM is derived from deeper soil profiles (Inamdar et al.,
374 2011), which is attributed to the sorption of aromatic DOM when subsurface flow water percolates through the soil profile.

375 Microbial degradation has been well-recognized as a critical factor in controlling organic material preservation in soils
376 (Barnes et al., 2018). Previous studies have reported a decreasing $\delta^{13}\text{C}_{\text{DOC}}$ with increasing DOC concentrations (Fig. 4) in
377 spring water (Nkoue Ndondo et al., 2020) and for TOC in soil profiles (Lloret et al., 2016; Nkoue Ndondo et al., 2020). This
378 can be explained by the lateral transport of DOC from microbially active soil horizons into rivers (Lambert et al., 2011),
379 resulting in the enhanced biodegradation of DOC with the preferential removal of ^{12}C . As a result, the remaining DOC with
380 lower concentrations is typically characterized by a heavier $\delta^{13}\text{C}_{\text{DOC}}$ (Nkoue Ndondo et al., 2020; Opsahl and Zepp, 2001),
381 which further indicates that the low-concentration DOC in the three rivers is the result of substantial microbial degradation.

382 Groundwater with significant SOC inputs due to highly active microbial activities has long been recognized as a
383 substantial source of DOC (McDonough et al., 2020; Shen et al., 2014). Several studies have reported increased groundwater
384 contributions with distance downstream at the watershed scale (Cowie et al., 2017; Iwasaki et al., 2021). The strong positive
385 relationship between conductivity and $\delta^{18}\text{O}$ ($p < 0.001$; Fig. S6a) is primarily due to the mixing of two end-members (i.e.,
386 high-conductivity with ^{18}O -enriched groundwater and low-conductivity with $\delta^{18}\text{O}$ -depleted headstream water) for river water
387 (Lamb, 2004), though it may also indicate the impact of evaporation in the catchment (Zhong et al., 2020). In addition, the

388 $\delta^{18}\text{O}$ values increased progressively from upstream to downstream (Fig. S6b), which also validates the two sources (i.e.,
389 headstream water and groundwater) of downstream river water, indicating that groundwater was likely an essential
390 contributor to downstream river water. This also supports our earlier hypothesis that aged DOC could be exported into rivers
391 through deeper water flow paths. However, groundwater was likely not the primary source of riverine DOC due to the
392 relatively low groundwater DOC concentrations as compared with riverine DOC concentrations (Fig. 2e; groundwater is
393 shown as “spring”). Moreover, the groundwater contribution was probably much less significant in the wet season (e.g.,
394 September in the study area), even in catchments where DOC is mainly derived from groundwater (Lloret et al., 2016). Thus,
395 we infer groundwater is an important but not a primary source of riverine DOC in the three study rivers.

396 **4.2 Anthropogenic impacts on DOC**

397 Previous research has found significant changes in DOC concentrations and DOM composition in agricultural and urban
398 landscapes (Spencer et al., 2019; Stanley et al., 2012). Conversion of native forest and pasture to row crop agriculture may
399 lead to substantial losses of SOC stores due to greatly accelerated erosion and decomposition rates (Guo and Gifford, 2002;
400 Montgomery, 2007; Stanley et al., 2012). In comparison, natural vegetation could greatly reduce SOC input into rivers by
401 effectively reducing soil erosion through the consolidation effect of roots on soil and the interception of rainfall by stems and
402 leaves (Zhang et al., 2019). Agricultural activities tend to liberate SOC through erosion over longer timescales and cause an
403 elevated DOC export into rivers (Figs. 4 and 6; Table 4), although DOC of urban origin can also make a massive
404 contribution to the riverine DOC pool (Sickman et al., 2007). Yet, anthropogenic impacts can also result in decreased DOC
405 concentrations globally due to reduced organic carbon inputs into soils and enhanced SOC decomposition induced by
406 warmer temperatures (Nagy et al., 2018; Spencer et al., 2019) or lead to undetectable changes in DOC concentrations (Veum
407 et al., 2009). These different responses are mainly due to diverse farming practices and associated changing effects on
408 terrestrial and aquatic carbon dynamics (Stanley et al., 2012).

409 Anthropogenic activities are important factors for the pervasive increase in nutrient and ion concentrations (Chetelat et
410 al., 2008; Smith and Schindler, 2009). For catchments without evaporite outcrops, their riverine Cl^- excluding atmospheric
411 contribution can be regarded as mainly of anthropogenic origin ($\text{Cl}^-_{\text{anthro}}$), which is a strong indicator of anthropogenic
412 activities (Fig. 6). The positive relationship between DOC concentrations and $\text{Cl}^-_{\text{anthro}}$ as shown in Fig. 4 also demonstrated
413 anthropogenic impacts on DOC export. Nutrient enrichment has been a well-known contributor to eutrophication (Paerl,
414 2009). In conjunction with increasing water residence time due to damming (Fig. 1a), our results demonstrate that enhanced
415 nutrient inputs into rivers will enhance algae production (Chen et al., 2021) and, eventually, accumulation of DOC (as
416 evidenced by the relationship between $\text{NH}_4^+\text{-N}$ and DOC in Fig. 4 with $\text{NH}_4^+\text{-N}$ serving as a predictor for DOC, see Table 4).
417 A recent study conducted in the Longtan Reservoir in the Xijiang River basin (China) with widespread karst landscape found

418 that a majority of its POC was intercepted or degraded within the reservoir, with the POC primarily originating from
419 phytoplankton (Yi et al., 2022). Its carbon isotope composition of POC ($\delta^{13}\text{C}_{\text{POC}}$) ranged from -35‰ to -30‰, which is
420 relatively depleted, and the POC was found to be a significant contributor to the reservoir's DOC (Yi et al., 2022). Thus, the
421 lower $\delta^{13}\text{C}_{\text{DOC}}$ with increasing NO_3^- -N further indicated the greater algae- or C3 plant-derived DOC accumulation with a
422 higher level of nutrients (Fig. 4 and Table 4).

423 Despite anthropogenic impacts on DOM characteristics and age have been widely proposed in the last two decades
424 (Butman et al., 2014; Coble et al., 2022; Zhou et al., 2021), there are no clear relationships between land use and ^{14}C ages in
425 our study area, which may result from large variations in soil characteristics and limited ^{14}C data. However, DOM
426 characteristics were found to be closely related to land use patterns (Figs. S4 and S5; Table 4). Although significant
427 relationships with urban and agricultural land uses were found for C1 and C2 (Table 4), it remains unclear how the
428 autochthonous contribution to riverine DOC pool varied with land use change because C1 and C2 are both likely derived
429 from autochthonous production but exhibit opposing trends with increasing urban and agricultural land uses. Overall DOM
430 in catchments with a higher proportion of urban and agricultural land uses were distinct from other catchments as it was less
431 aromatic (SUVA_{254} , Fig. 4), less recently produced (β/α , Fig. 4), and had a higher degree of humification (HIX, Fig. 4).
432 SUVA_{254} values for the three study rivers were comparable with those reported in coastal glacier mountainous streams with
433 late succession in southeast Alaska ($3.4 \pm 0.5 \text{ L mg}^{-1} \text{ m}^{-1}$, $n = 5$; Holt et al. 2021) and in the anthropogenic influenced
434 downstream of the Yangtze River ($3.4 \pm 1.1 \text{ L mg}^{-1} \text{ m}^{-1}$, $n = 82$; Zhou et al. 2021). Lower DOM aromaticity in the urban and
435 agricultural streams and rivers was consistent with previous studies (Hosen et al., 2014; Kadjeski et al., 2020), which
436 suggested a microbial origin for the DOM. However, it is important to note that this phenomenon was not universally
437 observed (Zhou et al., 2021). Furthermore, the less aromatic and less recently produced DOM could be due to soil organic
438 materials from deep soil profiles as a result of increased soil erosion by anthropogenic activities (Inamdar et al., 2011;
439 Stanley et al., 2012).

440 **4.3 Biogeochemical processes of DOC and comparison of $\Delta^{14}\text{C}_{\text{DOC}}$ in mountainous rivers**

441 In this study, geomorphologic characteristics and anthropogenic activities were identified as significant drivers of DOC
442 export and DOM composition across broad spatial scales. Here, we further examine how these two factors regulate the
443 biogeochemical processes of DOC. As discussed above, both geomorphology and anthropogenic activities are significant
444 factors controlling DOC concentrations. The PLS-PM analysis further revealed that the combined effects of the two factors
445 on DOC were mainly achieved through indirect influences on SOC content (Fig. 6). In contrast to the direct impact of
446 anthropogenic activities on SOC through soil erosion, the controls exerted by geomorphology on SOC were closely linked to
447 climate. Lower altitudes are typically associated with higher annual air temperatures (Fig. 4), which promote terrestrial net

448 primary production and the microbial degradation of soil OC (Voss et al., 2015), resulting in the accumulation of large
449 quantities of DOC in soils (Creed et al., 2018). Geomorphology is also associated with reduced water retention time due to
450 rapid flows, leading to a lower input of terrestrially-derived DOC into rivers as discussed earlier. It is worth noting that the
451 conversion of POC to DOC through dissolution and desorption (He et al., 2016) is also an important source of riverine DOC
452 (Fig. 6). Contrary to DOC concentrations, anthropogenic activities were identified as more effective predictors for DOM
453 characteristics than geomorphology (Table 4), highlighting the crucial role of anthropogenic activities in regulating DOM
454 dynamics. Therefore, the biogeochemical processes of DOM in the studied three rivers were collectively affected by
455 geomorphologic controls and anthropogenic impacts. Particularly, geomorphologic controls on DOM were mainly evidenced
456 by carbon isotopes, while anthropogenic impacts were primarily supported by the DOM fluorescence characteristics (Figs. 4
457 and Table 4). There was no significant relationship between carbon isotopes and optical properties, which is inconsistent
458 with previous studies (Aiken et al., 2014; Butman et al., 2012; Zhou et al., 2018). This discrepancy is likely due to the
459 potential masking effect of autochthonous DOM, as also evidenced by the decoupled relationship between $\Delta^{14}\text{C}_{\text{DOC}}$ and
460 SUVA_{254} in the St. Lawrence River (Aiken et al., 2014; Butman et al., 2012). Disentangling the dual influences
461 (geomorphologic and anthropogenic) is challenging because they have collectively affected both DOC concentration and
462 DOM quality in these rivers. A comprehensive assessment of the biogeochemical processes of DOC and their multiple
463 controlling factors will advance our understanding of riverine carbon cycling.

464 To provide a deeper insight into the DOC characteristics of the study rivers, DOC concentrations and the carbon isotopes of
465 DOC in global mountainous rivers are shown in Table 5. $\Delta^{14}\text{C}_{\text{DOC}}$ in the Yinjiang River ($-54.7 \pm 39.9 \text{‰}$; Tables 3 and 5) is
466 lower than that of the global average ($-11.5 \pm 134 \text{‰}$; Marwick et al., 2015), while similar to many other mountainous rivers
467 (e.g., the Mackenzie River) and small mountainous rivers in Puerto Rico; Moyer et al., 2013). $\Delta^{14}\text{C}_{\text{DOC}}$ values for the global
468 mountainous streams and rivers were shown by climate (according to the Köppen–Geiger climate classification (Beck et al.,
469 2018; Table 5) and ranged from tropical monsoon climate (Marwick et al., 2015), temperate oceanic climate (Evans et al.,
470 2007), cold semi-arid climates (Spencer et al., 2014) and continental subarctic climate (Hood et al., 2009). Fresh DOC in
471 mountainous rivers was reported across climates (Evans et al., 2007; Mayorga et al., 2005; Voss et al., 2022). In contrast, the
472 most aged DOC was observed in the Tibetan Plateau (Song et al., 2020; Spencer et al., 2014) and the Gulf of Alaska (Hood
473 et al., 2009). The riverine aged DOC from these regions with cold climates was mainly sourced from melting glaciers with
474 high bioavailability (Hood et al., 2009; Spencer et al., 2014) or derived from permafrost thaws in deeper soil horizons with
475 deeper flow paths (Song et al., 2020). As global air temperature increases, the greater input of the aged yet microbially labile
476 DOC into rivers would lead to increasing emissions of CO_2 and CH_4 , which in turn intensifies global warming (Vonk and
477 Gustafsson, 2013).

478

479 **Table 5.** Comparison of carbon isotopes of DOC in mountainous rivers worldwide.

Rivers/Region	Sampling Date (mmyyyy)	Climate	DOC (mg L ⁻¹)	$\delta^{13}\text{C}_{\text{DOC}}$ (‰)	$\Delta^{14}\text{C}_{\text{DOC}}$ (‰)	References
The Yinjiang River (China)	08/2018		1.3 ± 0.7	-26.6 ± 1.9	-55 ± 38	This study
Zambezi (Mozambique)	02/2012-04/2012		2.4 ± 0.6	-21.9 ± 2.4	64 ± 23	(Marwick et al., 2015)
Betsiboka (Madagascar)	01/2012-02/2012		1.3 ± 0.6	-22.8 ± 2.1	86 ± 43	
Amazon ^a	05/1995-10/1996	Tropical	1.9 ± 0.7	-26.0 ± 3.0	94 ± 176	(Mayorga et al., 2005)
Guanica and Fajardo (Puerto Rico)	09/2004-03/2008		2.3 ± 2.1	-26.1 ± 3.1	-55 ± 105	(Moyer et al., 2013)
North-West Australia (Australia)	05/2010 and 06/2011		1.5 ± 0.7	-25.0 ± 1.7	-67 ± 124	(Fellman et al., 2014)
Santa Clara (USA)	11/1997-03/1998		6.2 ± 2.7	-26.1 ± 0.9	-148 ± 58	(Masiello and Druffel, 2001)
Conwy (Wales) ^b		Temperate	9.2 ± 7.3	-28.0 ± 1.8	105 ± 6	(Evans et al., 2007)
Brocky Burn (Scotland)	02/1998 and 06/1998			-27.9 ± 0.2	29 ± 12	(Palmer et al., 2001)
Southeast Alaska	07/2013		0.8 ± 0.2	-27.0 ± 1.6	-93 ± 77	(Holt et al., 2021)
Gulf of Alaska	07/2008		1.2 ± 0.5	-23.9 ± 1.1	-207 ± 121	(Hood et al., 2009)
Alaska ^c	05/2012-10/2012		3.7 ± 4.1	-27.4 ± 0.8	-10 ± 55	(Behnke et al., 2020)
Kolyma (Russia) ^d	01/2003-12/2003			-28.5 ± 1.3	57 ± 51	(Neff et al., 2006)
Hudson (USA) ^e	01/2004		5.9 ± 0.7	-27.0 ± 0.0	-26 ± 13	(Raymond et al., 2004)
Central Ontario (Canada)	1990-1992	Continental	6.4 ± 4.5		96 ± 79	(Schiff et al., 1997)
Mackenzie River Basin (Canada) ^f	06/2018		4.3 ± 1.8	-26.9 ± 0.2	-55 ± 72	(Campeau et al., 2020)
Mulde (Germany)	08/2008-10/2010		9.8 ± 7.3	-26.6 ± 0.5	7 ± 27	(Tittel et al., 2013)
Fraser (Canada)	07/2009-05/2011		4.1 ± 5.6	-26.5 ± 0.5	58 ± 34	(Voss et al., 2022)
Yangtze River source region (China)	02/2017-12/2017		2.9 ± 1.4	-27.9 ± 3.3	-397 ± 185	(Song et al., 2020)
Tibetan Plateau (China)		Continental/Dry	0.27 ± 0.0	-23.5 ± 0.2	-209 ± 71	(Spencer et al., 2014)

480 ^a Only rivers draining mountainous areas from the Andean Cordillera were reported. ^b Data were obtained from Marwick et al. (2015). ^c
481 Calculated from mean values. ^d Only mountainous and upland rivers were reported. ^e Only the Upper Hudson River was reported. ^f Only
482 tributaries sourced from Cordillera were reported.

483 5 Conclusions

484 This study provided insights into the DOC dynamics and their influencing factors in anthropogenically-impacted subtropical
485 small mountainous rivers. Variations in DOC concentrations are regulated by both geomorphologic and anthropogenic
486 disturbances. We observed a positive relationship between DOC concentrations and anthropogenic land use but a negative
487 correlation between DOC concentration and catchment slope. Carbon isotope variations were mainly due to changing mean
488 catchment slope, while fluorescence properties of DOM were highly influenced by land use. Additionally, we found

489 increased aromaticity with elevated catchment slope and reduced agricultural and urban land uses, indicating the
490 geomorphologic and anthropogenic controls on DOM characteristics. We attribute these diverse DOC responses to altered
491 water retention time, SOC dynamics, and water flow paths. This study highlights that the combination of dual carbon
492 isotopes and optical properties are valuable tools in tracing the origin of riverine DOC and its in-stream processes. With
493 continued economic development and population growth, anthropogenic impacts on DOC are expected to be increasingly
494 evident. However, anthropogenic impacts may alter various biogeochemical processes of DOC in different catchments with
495 changing geomorphologic features due to complicated regulating mechanisms of organic carbon cycling, which to date
496 remains poorly understood. Further studies are warranted to fully understand the combined effects of local geomorphologic
497 controls and increasing anthropogenic impacts on DOC cycling.

498

499 *Data availability.* Data are available from the corresponding author Lishan Ran upon request at lsran@hku.hk.

500

501 *Author contributions.* JZ and SL conceived and designed the study. WW, JZ, and ZY contributed to the fieldwork. SC, WW,
502 YY and KMM contributed to the laboratory work and data analyses. SC wrote the original draft. LR, JZ and YY reviewed
503 and edited the manuscript.

504

505 *Competing interests.* The authors declare that they have no conflict of interest.

506

507 *Financial support.* This research was funded by the Strategic Priority Research Program of the Chinese Academy of
508 Sciences (XDB40000000), National Natural Science Foundation of China (Grant Nos. 41925002, 41422303 and 41803007),
509 and the Research Grants Council of Hong Kong (Grant No. 17300621).

510 **References**

511 Aiken G. R., Gilmour, C. C., Krabbenhoft, D. P. and Orem, W.: Dissolved organic matter in the Florida Everglades:
512 implications for ecosystem restoration, *Crit. Rev. Environ. Sci. Technol.*, 41, 217-248,
513 doi:10.1080/10643389.2010.530934, 2011.

514 Aiken G. R., Spencer, R. G. M., Striegl, R. G., Schuster, P. F. and Raymond, P. A.: Influences of glacier melt and permafrost
515 thaw on the age of dissolved organic carbon in the Yukon River basin, *Global Biogeochem. Cy.*, 28, 525-537,
516 doi:10.1002/2013gb004764, 2014.

517 Amaral V., Graeber, D., Calliari, D. and Alonso, C.: Strong linkages between DOM optical properties and main clades of
518 aquatic bacteria, *Limnol. Oceanogr.*, 61, 906-918, doi:10.1002/lno.10258, 2016.

519 Andersson C. A. and Bro, R.: The N-way toolbox for MATLAB, *Chemometr. intell. lab.*, 52, 1-4, 2000.

520 Ask J., Karlsson, J., Persson, L., Ask, P., Byström, P. and Jansson, M.: Terrestrial organic matter and light penetration:
521 Effects on bacterial and primary production in lakes, *Limnol. Oceanogr.*, 54, 2034-2040, doi:10.4319/lo.2009.54.6.2034,
522 2009.

523 Barnes R. T., Butman, D. E., Wilson, H. F. and Raymond, P. A.: Riverine Export of Aged Carbon Driven by Flow Path Depth
524 and Residence Time, *Environ. Sci. Technol.*, 52, 1028-1035, doi:10.1021/acs.est.7b04717, 2018.

525 Beck H. E., Zimmermann, N. E., McVicar, T. R., Vergopolan, N., Berg, A. and Wood, E. F.: Present and future
526 Koppen-Geiger climate classification maps at 1-km resolution, *Scientific Data*, 5, 180214, doi:10.1038/sdata.2018.214,
527 2018.

528 Behnke M. I., Stubbins, A., Fellman, J. B., Hood, E., Dittmar, T. and Spencer, R. G. M.: Dissolved organic matter sources in
529 glacierized watersheds delineated through compositional and carbon isotopic modeling, *Limnol. Oceanogr.*, 66, 438-451,
530 doi:10.1002/lno.11615, 2020.

531 Burt T. and Pinay, G.: Linking hydrology and biogeochemistry in complex landscapes, *Progress in Physical geography*, 29,
532 297-316, 2005.

533 Butman D. E., Wilson, H. F., Barnes, R. T., Xenopoulos, M. A. and Raymond, P. A.: Increased mobilization of aged carbon
534 to rivers by human disturbance, *Nat. Geosci.*, 8, 112-116, doi:10.1038/ngeo2322, 2014.

535 Butman D., Raymond, P. A., Butler, K. and Aiken, G.: Relationships between Delta C-14 and the molecular quality of
536 dissolved organic carbon in rivers draining to the coast from the conterminous United States, *Global Biogeochem. Cy.*, 26,
537 GB4014, doi:10.1029/2012GB004361, 2012.

538 Cai W. J.: Estuarine and coastal ocean carbon paradox: CO₂ sinks or sites of terrestrial carbon incineration?, *Annual Review*
539 *of Marine Science*, 3, 123-145, doi:10.1146/annurev-marine-120709-142723, 2011.

540 Campeau A., Soerensen, A., Martma, T., Åkerblom, S. and Zdanowicz, C.: Controls on the 14C-content of dissolved and
541 particulate organic carbon mobilized across the Mackenzie River basin, Canada, *Global Biogeochem. Cy.*,
542 doi:10.1029/2020gb006671, 2020.

543 Catalán N., Marcé, R., Kothawala, D. N. and Tranvik, L. J.: Organic carbon decomposition rates controlled by water
544 retention time across inland waters, *Nat. Geosci.*, 9, 501-504, doi:10.1038/ngeo2720, 2016.

545 Chen S., Zhong, J., Li, C., Wang, W.-f., Xu, S., Yan, Z.-l. and Li, S.-l.: The chemical weathering characteristics of different
546 lithologic mixed small watersheds in Southwest China, *Chinese J. Ecol.*, 39, 1288-1299 (in Chinese with English abstract),
547 2020.

548 Chen S., Zhong, J., Li, S., Ran, L., Wang, W., Xu, S., Yan, Z. and Xu, S.: Multiple controls on carbon dynamics in mixed
549 karst and non-karst mountainous rivers, Southwest China, revealed by carbon isotopes ($\delta^{13}\text{C}$ and $\Delta^{14}\text{C}$), *Sci.*
550 *Total Environ.*, 791, 148347, doi:10.1016/j.scitotenv.2021.148347, 2021.

551 Chetelat B., Liu, C.-Q., Zhao, Z., Wang, Q., Li, S., Li, J. and Wang, B.: Geochemistry of the dissolved load of the
552 Changjiang Basin rivers: anthropogenic impacts and chemical weathering, *Geochim. Cosmochim. Acta*, 72, 4254-4277,
553 2008.

554 Coble A. A., Wymore, A. S., Potter, J. D. and McDowell, W. H.: Land Use Overrides Stream Order and Season in Driving
555 Dissolved Organic Matter Dynamics Throughout the Year in a River Network, *Environ. Sci. Technol.*, 56, 2009-2020,
556 doi:10.1021/acs.est.1c06305, 2022.

557 Connolly C. T., Khosh, M. S., Burkart, G. A., Douglas, T. A., Holmes, R. M., Jacobson, A. D., Tank, S. E. and McClelland, J.
558 W.: Watershed slope as a predictor of fluvial dissolved organic matter and nitrate concentrations across geographical space
559 and catchment size in the Arctic, *Environ. Res. Lett.*, 13, 104015, doi:10.1088/1748-9326/aae35d, 2018.

560 Cowie R. M., Knowles, J. F., Dailey, K. R., Williams, M. W., Mills, T. J. and Molotch, N. P.: Sources of streamflow along a
561 headwater catchment elevational gradient, *J. Hydrol.*, 549, 163-178, doi:10.1016/j.jhydrol.2017.03.044, 2017.

562 Creed I. F., Bergstrom, A. K., Trick, C. G., Grimm, N. B., Hessen, D. O., Karlsson, J., Kidd, K. A., Kritzbeg, E., McKnight,
563 D. M., Freeman, E. C., Senar, O. E., Andersson, A., Ask, J., Berggren, M., Cherif, M., Giesler, R., Hotchkiss, E. R.,
564 Kortelainen, P., Palta, M. M., Vrede, T. and Weyhenmeyer, G. A.: Global change-driven effects on dissolved organic
565 matter composition: Implications for food webs of northern lakes, *Global Change Biol.*, 24, 3692-3714,
566 doi:10.1111/gcb.14129, 2018.

567 DeFrancesco C. and Guéguen, C.: Long-term Trends in Dissolved Organic Matter Composition and Its Relation to Sea Ice in
568 the Canada Basin, Arctic Ocean (2007–2017), *Journal of Geophysical Research: Oceans*, 126, doi:10.1029/2020jc016578,
569 2021.

570 Devesa-Rey R. and Barral, M. T.: Allochthonous versus autochthonous naturally occurring organic matter in the Anllóns
571 river bed sediments (Spain), *Environmental Earth Sciences*, 66, 773-782, doi:10.1007/s12665-011-1286-3, 2011.

572 Dong K., Lang, Y., Hu, N., Zhong, J., Xu, S., Hauser, T.-M. and Gan, R.: The new AMS facility at Tianjin University,
573 *Radiation Detection Technology and Methods*, 2, doi:10.1007/s41605-018-0064-0, 2018.

574 Du Y., Chen, F., Zhang, Y., He, H., Wen, S., Huang, X., Song, C., Li, K., Wang, J., Keellings, D. and Lu, Y.: Human Activity
575 Coupled With Climate Change Strengthens the Role of Lakes as an Active Pipe of Dissolved Organic Matter, *Earth's*
576 *Future*, 11, doi:10.1029/2022ef003412, 2023.

577 Du Y., Zhang, Q., Liu, Z., He, H., Lurling, M., Chen, M. and Zhang, Y.: Composition of dissolved organic matter controls
578 interactions with La and Al ions: Implications for phosphorus immobilization in eutrophic lakes, *Environ. Pollut.*, 248,
579 36-47, doi:10.1016/j.envpol.2019.02.002, 2019.

580 Evans C. D., Freeman, C., Cork, L. G., Thomas, D. N., Reynolds, B., Billett, M. F., Garnett, M. H. and Norris, D.: Evidence
581 against recent climate-induced destabilisation of soil carbon from ¹⁴C analysis of riverine dissolved organic matter,
582 *Geophys. Res. Lett.*, 34, doi:10.1029/2007gl029431, 2007.

583 Fasching C., Akotoye, C., Bižić, M., Fonvielle, J., Ionescu, D., Mathavarajah, S., Zoccarato, L., Walsh, D. A., Grossart, H. P.
584 and Xenopoulos, M. A.: Linking stream microbial community functional genes to dissolved organic matter and inorganic
585 nutrients, *Limnol. Oceanogr.*, 65, doi:10.1002/lno.11356, 2019.

586 Fasching C., Ulseth, A. J., Schelker, J., Steniczka, G. and Battin, T. J.: Hydrology controls dissolved organic matter export
587 and composition in an Alpine stream and its hyporheic zone, *Limnol. Oceanogr.*, 61, 558-571, doi:10.1002/lno.10232,
588 2016.

589 Fellman J. B., Hood, E. and Spencer, R. G. J. L.: Fluorescence spectroscopy opens new windows into dissolved organic
590 matter dynamics in freshwater ecosystems: A review, *Limnol. Oceanogr.*, 55, 2452-2462, doi:10.4319/lo.2010.55.6.2452,
591 2010.

592 Fellman J. B., Spencer, R. G., Raymond, P. A., Pettit, N. E., Skrzypek, G., Hernes, P. J. and Grierson, P. F.: Dissolved organic
593 carbon biolability decreases along with its modernization in fluvial networks in an ancient landscape, *Ecology*, 95,
594 2622-2632, 2014.

595 Findlay S., Sinsabaugh, R. L., Fischer, D. T. and Franchini, P.: Sources of dissolved organic carbon supporting planktonic
596 bacterial production in the tidal freshwater Hudson River, *Ecosystems*, 1, 227-239, 1998.

597 Gaillardet J., Dupre, B., Allegre, C. J. and Négrel, P.: Chemical and physical denudation in the Amazon River Basin, *Chem.*
598 *Geol.*, 142, 141-173, 1997.

599 Guo L. B. and Gifford, R. M.: Soil carbon stocks and land use change: a meta analysis, *Global Change Biol.*, 8, 345-360,
600 doi:10.1046/j.1354-1013.2002.00486.x, 2002.

601 Han G. and Liu, C.-Q.: Water geochemistry controlled by carbonate dissolution: a study of the river waters draining
602 karst-dominated terrain, Guizhou Province, China, *Chem. Geol.*, 204, 1-21, doi:10.1016/j.chemgeo.2003.09.009, 2004.

603 Harms T. K., Edmonds, J. W., Genet, H., Creed, I. F., Aldred, D., Balsler, A. and Jones, J. B.: Catchment influence on nitrate
604 and dissolved organic matter in Alaskan streams across a latitudinal gradient, *J. Geophys. Res.: Biogeo.*, 121, 350-369,
605 doi:10.1002/2015jg003201, 2016.

606 He W., Chen, M., Schlautman, M. A. and Hur, J.: Dynamic exchanges between DOM and POM pools in coastal and inland
607 aquatic ecosystems: A review, *Sci. Total Environ.*, 551-552, 415-428, doi:10.1016/j.scitotenv.2016.02.031, 2016.

608 Hengl T., de Jesus, J. M., MacMillan, R. A., Batjes, N. H., Heuvelink, G. B., Ribeiro, E., Samuel-Rosa, A., Kempen, B.,
609 Leenaars, J. G., Walsh, M. G. and Gonzalez, M. R.: SoilGrids1km--global soil information based on automated mapping,
610 *PLoS One*, 9, e105992, doi:10.1371/journal.pone.0105992, 2014.

611 Holt A. D., Fellman, J., Hood, E., Kellerman, A. M., Raymond, P., Stubbins, A., Dittmar, T. and Spencer, R. G. M.: The
612 evolution of stream dissolved organic matter composition following glacier retreat in coastal watersheds of southeast
613 Alaska, *Biogeochemistry*, doi:10.1007/s10533-021-00815-6, 2021.

614 Hood E., Fellman, J., Spencer, R. G., Hernes, P. J., Edwards, R., D'Amore, D. and Scott, D.: Glaciers as a source of ancient
615 and labile organic matter to the marine environment, *Nature*, 462, 1044-1047, doi:10.1038/nature08580, 2009.

616 Hood E., Gooseff, M. N. and Johnson, S. L.: Changes in the character of stream water dissolved organic carbon during

617 flushing in three small watersheds, Oregon, *J. Geophys. Res.: Biogeo.*, 111, doi:10.1029/2005JG000082, 2006.

618 Hosen J. D., McDonough, O. T., Febria, C. M. and Palmer, M. A.: Dissolved organic matter quality and bioavailability
619 changes across an urbanization gradient in headwater streams, *Environ. Sci. Technol.*, 48, 7817-7824,
620 doi:10.1021/es501422z, 2014.

621 Inamdar S., Singh, S., Dutta, S., Levia, D., Mitchell, M., Scott, D., Bais, H. and McHale, P.: Fluorescence characteristics and
622 sources of dissolved organic matter for stream water during storm events in a forested mid-Atlantic watershed, *J. Geophys.
623 Res.: Biogeo.*, 116, doi:10.1029/2011jg001735, 2011.

624 Inamdar S.: The use of geochemical mixing models to derive runoff sources and hydrologic flow paths, *Forest hydrology
625 and biogeochemistry*. Springer, pp. 163-183, 2011

626 Iwasaki K., Nagasaka, Y. and Nagasaka, A.: Geological Effects on the Scaling Relationships of Groundwater Contributions
627 in Forested Watersheds, *Water Resour. Res.*, 57, doi:10.1029/2021wr029641, 2021.

628 Kadjeski M., Fasching, C. and Xenopoulos, M. A.: Synchronous Biodegradability and Production of Dissolved Organic
629 Matter in Two Streams of Varying Land Use, *Front. Microbiol.*, 11, 568629, doi:10.3389/fmicb.2020.568629, 2020.

630 Kim J., Kim, Y., Park, S. E., Kim, T. H., Kim, B. G., Kang, D. J. and Rho, T.: Impact of aquaculture on distribution of
631 dissolved organic matter in coastal Jeju Island, Korea, based on absorption and fluorescence spectroscopy, *Environ Sci
632 Pollut Res Int*, 29, 553-563, doi:10.1007/s11356-021-15553-3, 2022.

633 Lambert T., Bouillon, S., Darchambeau, F., Morana, C., Roland, F. A. E., Descy, J.-P. and Borges, A. V.: Effects of human
634 land use on the terrestrial and aquatic sources of fluvial organic matter in a temperate river basin (The Meuse River,
635 Belgium), *Biogeochemistry*, 136, 191-211, doi:10.1007/s10533-017-0387-9, 2017.

636 Lambert T., Perolo, P., Escoffier, N. and Perga, M.-E.: Enhanced bioavailability of dissolved organic matter (DOM) in
637 human-disturbed streams in Alpine fluvial networks, *Biogeosciences*, 19, 187-200, doi:10.5194/bg-19-187-2022, 2022.

638 Lambert T., Pierson-Wickmann, A.-C., Gruau, G., Thibault, J.-N. and Jaffrezic, A.: Carbon isotopes as tracers of dissolved
639 organic carbon sources and water pathways in headwater catchments, *J. Hydrol.*, 402, 228-238,
640 doi:10.1016/j.jhydrol.2011.03.014, 2011.

641 Lambs L.: Interactions between groundwater and surface water at river banks and the confluence of rivers, *J. Hydrol.*, 288,
642 312-326, doi:10.1016/j.jhydrol.2003.10.013, 2004.

643 Lee L.-C., Hsu, T.-C., Lee, T.-Y., Shih, Y.-T., Lin, C.-Y., Jien, S.-H., Hein, T., Zehetner, F., Shiah, F.-K. and Huang, J.-C.:
644 Unusual roles of discharge, slope and soc in doc transport in small mountainous rivers, Taiwan, *Sci. Rep.*, 9, 41422303,
645 doi:10.1038/s41598-018-38276-x, 2019.

646 Leithold E. L., Blair, N. E. and Perkey, D. W.: Geomorphologic controls on the age of particulate organic carbon from small
647 mountainous and upland rivers, *Global Biogeochem. Cy.*, 20, GB3022, doi:10.1029/2005gb002677, 2006.

648 Leonard A., Castle, S., Burr, G. S., Lange, T. and Thomas, J.: A Wet Oxidation Method for AMS Radiocarbon Analysis of
649 Dissolved Organic Carbon in Water, *Radiocarbon*, 55, 545-552, doi:10.1017/S0033822200057672, 2013.

650 Li P., Lee, S. H., Lee, S. H., Lee, J. B., Lee, Y. K., Shin, H. S. and Hur, J.: Seasonal and storm-driven changes in chemical
651 composition of dissolved organic matter: a case study of a reservoir and its forested tributaries, *Environ Sci Pollut Res Int*,
652 23, 24834-24845, doi:10.1007/s11356-016-7720-z, 2016.

653 Li Yung Lung J. Y. S., Tank, S. E., Spence, C., Yang, D., Bonsal, B., McClelland, J. W. and Holmes, R. M.: Seasonal and
654 Geographic Variation in Dissolved Carbon Biogeochemistry of Rivers Draining to the Canadian Arctic Ocean and Hudson
655 Bay, *J. Geophys. Res.: Biogeo.*, 123, 3371-3386, doi:10.1029/2018jg004659, 2018.

656 Lloret E., Dessert, C., Buss, H. L., Chaduteau, C., Huon, S., Alberic, P. and Benedetti, M. F.: Sources of dissolved organic
657 carbon in small volcanic mountainous tropical rivers, examples from Guadeloupe (French West Indies), *Geoderma*, 282,
658 129-138, doi:10.1016/j.geoderma.2016.07.014, 2016.

659 Marwick T. R., Tamooch, F., Teodoru, C. R., Borges, A. V., Darchambeau, F. and Bouillon, S.: The age of river-transported
660 carbon: A global perspective, *Global Biogeochem. Cy.*, 29, 122-137, doi:10.1002/2014GB004911, 2015.

661 Masiello C. A. and Druffel, E. R.: Carbon isotope geochemistry of the Santa Clara River, *Global Biogeochem. Cy.*, 15,
662 407-416, 2001.

663 Mayorga E., Aufdenkampe, A. K., Masiello, C. A., Krusche, A. V., Hedges, J. I., Quay, P. D., Richey, J. E. and Brown, T. A.:

664 Young organic matter as a source of carbon dioxide outgassing from Amazonian rivers, *Nature*, 436, 538-541,
665 doi:10.1038/nature03880, 2005.

666 McDonough L. K., Santos, I. R., Andersen, M. S., O'Carroll, D. M., Rutledge, H., Meredith, K., Oudone, P., Bridgeman, J.,
667 Goody, D. C., Sorensen, J. P. R., Lapworth, D. J., MacDonald, A. M., Ward, J. and Baker, A.: Changes in global
668 groundwater organic carbon driven by climate change and urbanization, *Nat. Commun.*, 11, 1279,
669 doi:10.1038/s41467-020-14946-1, 2020.

670 McGuire K. J., McDonnell, J. J., Weiler, M., Kendall, C., McGlynn, B. L., Welker, J. M. and Seibert, J.: The role of
671 topography on catchment-scale water residence time, *Water Resour. Res.*, 41, doi:10.1029/2004wr003657, 2005.

672 McKnight D. M., Boyer, E. W., Westerhoff, P. K., Doran, P. T., Kulbe, T. and Andersen, D. T.: Spectrofluorometric
673 characterization of dissolved organic matter for indication of precursor organic material and aromaticity, *Limnol.*
674 *Oceanogr.*, 46, 38-48, doi:10.4319/lo.2001.46.1.0038, 2001.

675 Meybeck M.: Atmospheric inputs and river transport of dissolved substances, *Dissolved loads of rivers surface water*
676 *quantity/quality relationships*, pp. 173-192, 1983

677 Mineau M. M., Wollheim, W. M., Buffam, I., Findlay, S. E. G., Hall, R. O., Hotchkiss, E. R., Koenig, L. E., McDowell, W. H.
678 and Parr, T. B.: Dissolved organic carbon uptake in streams: A review and assessment of reach-scale measurements, *J.*
679 *Geophys. Res.: Biogeo.*, 121, 2019-2029, doi:10.1002/2015jg003204, 2016.

680 Minor E. C., Swenson, M. M., Mattson, B. M. and Oyler, A. R.: Structural characterization of dissolved organic matter: a
681 review of current techniques for isolation and analysis, *Environ. Sci.: Processes Impacts*, 16, 2064-2079,
682 doi:10.1039/c4em00062e, 2014.

683 Montgomery D. R.: Soil erosion and agricultural sustainability, *Proc. Natl. Acad. Sci. USA*, 104, 13268-13272,
684 doi:10.1073/pnas.0611508104, 2007.

685 Mostofa K. M. G., Jie, Y., Sakugawa, H. and Liu, C. Q.: Equal Treatment of Different EEM Data on PARAFAC Modeling
686 Produces Artifact Fluorescent Components That Have Misleading Biogeochemical Consequences, *Environ. Sci. Technol.*,
687 53, 561-563, doi:10.1021/acs.est.8b06647, 2019.

688 Moyer R. P., Bauer, J. E. and Grotoli, A. G.: Carbon isotope biogeochemistry of tropical small mountainous river, estuarine,
689 and coastal systems of Puerto Rico, *Biogeochemistry*, 112, 589-612, doi:10.1007/s10533-012-9751-y, 2013.

690 Murphy K. R., Stedmon, C. A., Wenig, P. and Bro, R.: OpenFluor—an online spectral library of auto-fluorescence by organic
691 compounds in the environment, *Analytical Methods*, 6, 658-661, 2014.

692 Mzobe P., Yan, Y., Berggren, M., Pilesjö, P., Olefeldt, D., Lundin, E., Roulet, N. T. and Persson, A.: Morphometric Control
693 on Dissolved Organic Carbon in Subarctic Streams, *J. Geophys. Res.: Biogeo.*, 125, e2019JG005348,
694 doi:10.1029/2019jg005348, 2020.

695 Nagy R. C., Porder, S., Brando, P., Davidson, E. A., Figueira, A., Neill, C., Riskin, S. and Trumbore, S.: Soil Carbon
696 Dynamics in Soybean Cropland and Forests in Mato Grosso, Brazil, *J Geophys Res Biogeosci*, 123, 18-31,
697 doi:10.1002/2017JG004269, 2018.

698 Neff J. C., Finlay, J. C., Zimov, S. A., Davydov, S. P., Carrasco, J. J., Schuur, E. A. G. and Davydova, A. I.: Seasonal changes
699 in the age and structure of dissolved organic carbon in Siberian rivers and streams, *Geophys. Res. Lett.*, 33,
700 doi:10.1029/2006gl028222, 2006.

701 Nkoue Ndong G. R., Probst, J. L., Ndjama, J., Ndam Ngoupayou, J. R., Boeglin, J. L., Takem, G. E., Brunet, F., Mortatti, J.,
702 Gauthier-Lafaye, F., Braun, J. J. and Ekodeck, G. E.: Stable Carbon Isotopes $\delta^{13}\text{C}$ as a Proxy for Characterizing Carbon
703 Sources and Processes in a Small Tropical Headwater Catchment: Nsimi, Cameroon, *Aquat. Geochem.*, 27, 1-30,
704 doi:10.1007/s10498-020-09386-8, 2020.

705 Ohno T.: Fluorescence inner-filtering correction for determining the humification index of dissolved organic matter, *Environ.*
706 *Sci. Technol.*, 36, 742-746, doi:10.1021/es0155276, 2002.

707 Opsahl S. P. and Zepp, R. G.: Photochemically-induced alteration of stable carbon isotope ratios ($\delta^{13}\text{C}$) in terrigenous
708 dissolved organic carbon, *Geophys. Res. Lett.*, 28, 2417-2420, doi:10.1029/2000gl012686, 2001.

709 Paerl H. W.: Controlling Eutrophication along the Freshwater–Marine Continuum: Dual Nutrient (N and P) Reductions are
710 Essential, *Estuar. and Coast.*, 32, 593-601, doi:10.1007/s12237-009-9158-8, 2009.

711 Palmer S. M., Hope, D., Billett, M. F., Dawson, J. J. and Bryant, C. L.: Sources of organic and inorganic carbon in a
712 headwater stream: evidence from carbon isotope studies, *Biogeochemistry*, 52, 321-338, 2001.

713 Parlanti E., Wörz, K., Geoffroy, L. and Lamotte, M.: Dissolved organic matter fluorescence spectroscopy as a tool to
714 estimate biological activity in a coastal zone submitted to anthropogenic inputs, *Org. Geochem.*, 31, 1765-1781,
715 doi:10.1016/S0146-6380(00)00124-8, 2000.

716 Poulin B. A., Ryan, J. N. and Aiken, G. R.: Effects of iron on optical properties of dissolved organic matter, *Environ. Sci.*
717 *Technol.*, 48, 10098-10106, doi:10.1021/es502670r, 2014.

718 Quinton J. N., Govers, G., Van Oost, K. and Bardgett, R. D.: The impact of agricultural soil erosion on biogeochemical
719 cycling, *Nat. Geosci.*, 3, 311-314, doi:10.1038/ngeo838, 2010.

720 Ramos M. C., Quinton, J. N. and Tyrrel, S. F.: Effects of cattle manure on erosion rates and runoff water pollution by faecal
721 coliforms, *J. Environ. Manage.*, 78, 97-101, doi:10.1016/j.jenvman.2005.04.010, 2006.

722 Rawlins M. A., Connolly, C. T. and McClelland, J. W.: Modeling Terrestrial Dissolved Organic Carbon Loading to Western
723 Arctic Rivers, *J. Geophys. Res.: Biogeo.*, doi:10.1029/2021jg006420, 2021.

724 Raymond P. A. and Spencer, R. G. M.: Chapter 11 - Riverine DOM, in: Hansell, D.A., Carlson, C.A. (Eds.),
725 *Biogeochemistry of Marine Dissolved Organic Matter (Second Edition)*. Academic Press, Boston, pp. 509-533, 2015

726 Raymond P. A., Bauer, J. E., Caraco, N. F., Cole, J. J., Longworth, B. and Petsch, S. T.: Controls on the variability of organic
727 matter and dissolved inorganic carbon ages in northeast US rivers, *Mar. Chem.*, 92, 353-366,
728 doi:10.1016/j.marchem.2004.06.036, 2004.

729 Raymond P. A., Hartmann, J., Lauerwald, R., Sobek, S., McDonald, C., Hoover, M., Butman, D., Striegl, R., Mayorga, E.,
730 Humborg, C., Kortelainen, P., Durr, H., Meybeck, M., Ciais, P. and Guth, P.: Global carbon dioxide emissions from inland
731 waters, *Nature*, 503, 355-359, doi:10.1038/nature12760, 2013.

732 Ryan K. A., Palacios, L. C., Encina, F., Graeber, D., Osorio, S., Stubbins, A., Woelfl, S. and Nimptsch, J.: Assessing inputs of
733 aquaculture-derived nutrients to streams using dissolved organic matter fluorescence, *Sci. Total Environ.*, 807, 150785,
734 doi:10.1016/j.scitotenv.2021.150785, 2022.

735 Sanchez G.: *PLS path modeling with R*, Berkeley: Trowchez Editions, 383, 551, 2013.

736 Schiff S. L., Aravena, R., Trumbore, S. E., Hinton, M. J., Elgood, R. and Dillon, P. J.: Export of DOC from forested
737 catchments on the Precambrian Shield of Central Ontario: Clues from ¹³C and ¹⁴C, *Biogeochemistry*, 36, 43-65, 1997.

738 Shen Y., Chapelle, F. H., Strom, E. W. and Benner, R.: Origins and bioavailability of dissolved organic matter in groundwater,
739 *Biogeochemistry*, 122, 61-78, doi:10.1007/s10533-014-0029-4, 2014.

740 Shutova Y., Baker, A., Bridgeman, J. and Henderson, R. K.: Spectroscopic characterisation of dissolved organic matter
741 changes in drinking water treatment: From PARAFAC analysis to online monitoring wavelengths, *Water Res.*, 54, 159-169,
742 doi:10.1016/j.watres.2014.01.053, 2014.

743 Sickman J. O., Zanoli, M. J. and Mann, H. L.: Effects of Urbanization on Organic Carbon Loads in the Sacramento River,
744 California, *Water Resour. Res.*, 43, doi:10.1029/2007wr005954, 2007.

745 Smith V. H. and Schindler, D. W.: Eutrophication science: where do we go from here?, *Trends Ecol. Evol.*, 24, 201-207,
746 doi:10.1016/j.tree.2008.11.009, 2009.

747 Song C., Wang, G., Haghpor, N. and Raymond, P. A.: Warming and monsoonal climate lead to large export of
748 millennial-aged carbon from permafrost catchments of the Qinghai-Tibet Plateau, *Environ. Res. Lett.*, 15,
749 doi:10.1088/1748-9326/ab83ac, 2020.

750 Spencer R. G. M., Guo, W., Raymond, P. A., Dittmar, T., Hood, E., Fellman, J. and Stubbins, A.: Source and biolability of
751 ancient dissolved organic matter in glacier and lake ecosystems on the Tibetan Plateau, *Geochim. Cosmochim. Acta*, 142,
752 64-74, doi:10.1016/j.gca.2014.08.006, 2014.

753 Spencer R. G. M., Kellerman, A. M., Podgorski, D. C., Macedo, M. N., Jankowski, K., Nunes, D. and Neill, C.: Identifying
754 the Molecular Signatures of Agricultural Expansion in Amazonian Headwater Streams, *J. Geophys. Res.: Biogeo.*, 124,
755 1637-1650, doi:10.1029/2018jg004910, 2019.

756 Stanley E. H., Powers, S. M., Lottig, N. R., Buffam, I. and Crawford, J. T.: Contemporary changes in dissolved organic
757 carbon (DOC) in human-dominated rivers: is there a role for DOC management?, *Freshwat. Biol.*, 57, 26-42,

758 doi:10.1111/j.1365-2427.2011.02613.x, 2012.

759 Stedmon C. A. and Bro, R.: Characterizing dissolved organic matter fluorescence with parallel factor analysis: a tutorial,
760 *Limnol. Oceanogr. Methods*, 6, 572-579, doi:10.4319/lom.2008.6.572, 2008.

761 Tian J., Dungait, J. A. J., Lu, X., Yang, Y., Hartley, I. P., Zhang, W., Mo, J., Yu, G., Zhou, J. and Kuzyakov, Y.: Long-term
762 nitrogen addition modifies microbial composition and functions for slow carbon cycling and increased sequestration in
763 tropical forest soil, *Glob Chang Biol*, 25, 3267-3281, doi:10.1111/gcb.14750, 2019.

764 Tittel J., Büttner, O., Freier, K., Heiser, A., Sudbrack, R. and Ollesch, G.: The age of terrestrial carbon export and rainfall
765 intensity in a temperate river headwater system, *Biogeochemistry*, 115, 53-63, doi:10.1007/s10533-013-9896-3, 2013.

766 Tiwari T., Laudon, H., Beven, K. and Ågren, A. M.: Downstream changes in DOC: Inferring contributions in the face of
767 model uncertainties, *Water Resour. Res.*, 50, 514-525, doi:10.1002/2013wr014275, 2014.

768 Toming K., Tuvikene, L., Vilbaste, S., Agasild, H., Viik, M., Kisand, A., Feldmann, T., Martma, T., Jones, R. I. and Nõges, T.:
769 Contributions of autochthonous and allochthonous sources to dissolved organic matter in a large, shallow, eutrophic lake
770 with a highly calcareous catchment, *Limnol. Oceanogr.*, 58, 1259-1270, doi:10.4319/lo.2013.58.4.1259, 2013.

771 Veum K. S., Goyne, K. W., Motavalli, P. P. and Udawatta, R. P.: Runoff and dissolved organic carbon loss from a
772 paired-watershed study of three adjacent agricultural Watersheds, *Agric., Ecosyst. Environ.*, 130, 115-122,
773 doi:10.1016/j.agee.2008.12.006, 2009.

774 Vonk J. E. and Gustafsson, Ö.: Permafrost-carbon complexities, *Nat. Geosci.*, 6, 675-676, doi:10.1038/ngeo1937, 2013.

775 Voss B. M., Eglinton, T. I., Peucker-Ehrenbrink, B., Galy, V., Lang, S. Q., McIntyre, C., Spencer, R. G. M., Bulygina, E.,
776 Wang, Z. A. and Guay, K. A.: Isotopic evidence for sources of dissolved carbon and the role of organic matter respiration
777 in the Fraser River basin, Canada, *Biogeochemistry*, doi:10.1007/s10533-022-00945-5, 2022.

778 Voss B. M., Peucker-Ehrenbrink, B., Eglinton, T. I., Spencer, R. G. M., Bulygina, E., Galy, V., Lamborg, C. H., Ganguli, P.
779 M., Montluçon, D. B., Marsh, S., Gillies, S. L., Fanslau, J., Epp, A. and Luymes, R.: Seasonal hydrology drives rapid
780 shifts in the flux and composition of dissolved and particulate organic carbon and major and trace ions in the Fraser River,
781 Canada, *Biogeosciences*, 12, 5597-5618, doi:10.5194/bg-12-5597-2015, 2015.

782 Walker S. A., Amon, R. M. W., Stedmon, C., Duan, S. and Louchouart, P.: The use of PARAFAC modeling to trace
783 terrestrial dissolved organic matter and fingerprint water masses in coastal Canadian Arctic surface waters, *Journal of*
784 *Geophysical Research*, 114, doi:10.1029/2009jg000990, 2009.

785 Wang J., Walter, B. A., Yao, F., Song, C., Ding, M., Maroof, A. S., Zhu, J., Fan, C., McAlister, J. M., Sikder, S., Sheng, Y.,
786 Allen, G. H., Crétau, J.-F. and Wada, Y.: GeoDAR: georeferenced global dams and reservoirs dataset for bridging
787 attributes and geolocations, *Earth System Science Data*, 14, 1869-1899, doi:10.5194/essd-14-1869-2022, 2022.

788 Weishaar J. L., Aiken, G. R., Bergamaschi, B. A., Fram, M. S., Fujii, R. and Mopper, K.: Evaluation of specific ultraviolet
789 absorbance as an indicator of the chemical composition and reactivity of dissolved organic carbon, *Environ. Sci. Technol.*,
790 37, 4702-4708, 2003.

791 Williams C. J., Frost, P. C., Morales-Williams, A. M., Larson, J. H., Richardson, W. B., Chiandet, A. S. and Xenopoulos, M.
792 A.: Human activities cause distinct dissolved organic matter composition across freshwater ecosystems, *Global Change*
793 *Biol.*, 22, 613-626, doi:10.1111/gcb.13094, 2016.

794 Williams C. J., Yamashita, Y., Wilson, H. F., Jaffé, R. and Xenopoulos, M. A.: Unraveling the role of land use and microbial
795 activity in shaping dissolved organic matter characteristics in stream ecosystems, *Limnol. Oceanogr.*, 55, 1159-1171,
796 doi:10.4319/lo.2010.55.3.1159, 2010.

797 Wilson H. F. and Xenopoulos, M. A.: Effects of agricultural land use on the composition of fluvial dissolved organic matter,
798 *Nat. Geosci.*, 2, 37-41, doi:10.1038/ngeo391, 2008.

799 Xenopoulos M. A., Barnes, R. T., Boodoo, K. S., Butman, D., Catalán, N., D'Amario, S. C., Fasching, C., Kothawala, D. N.,
800 Pisani, O., Solomon, C. T., Spencer, R. G. M., Williams, C. J. and Wilson, H. F.: How humans alter dissolved organic
801 matter composition in freshwater: relevance for the Earth's biogeochemistry, *Biogeochemistry*, 1-26,
802 doi:10.1007/s10533-021-00753-3, 2021.

803 Yi Y., Li, S.-L., Zhong, J., Wang, W., Chen, S., Bao, H. and He, D.: The influence of the deep subtropical reservoir on the
804 karstic riverine carbon cycle and its regulatory factors: Insights from the seasonal and hydrological changes, *Water Res.*,

805 226, doi:10.1016/j.watres.2022.119267, 2022.

806 Yi Y., Zhong, J., Bao, H., Mostofa, K. M. G., Xu, S., Xiao, H.-Y. and Li, S.-L.: The impacts of reservoirs on the sources and
807 transport of riverine organic carbon in the karst area: a multi-tracer study, *Water Res.*, 194, 116933,
808 doi:10.1016/j.watres.2021.116933, 2021.

809 Zhang Q., Tao, Z., Ma, Z., Gao, Q., Deng, H., Xu, P., Ding, J., Wang, Z. and Lin, Y.: Hydro-ecological controls on riverine
810 organic carbon dynamics in the tropical monsoon region, *Sci. Rep.*, 9, 11871, doi:10.1038/s41598-019-48208-y, 2019.

811 Zhong J., Chen, S., Wang, W., Yan, Z., Ellam, R. M. and Li, S. L.: Unravelling the hydrological effects on spatiotemporal
812 variability of water chemistry in mountainous rivers from Southwest China, *Hydrol. Process.*, 34, 5595-5605,
813 doi:10.1002/hyp.13980, 2020.

814 Zhong J., Li, S.-L., Zhu, X., Liu, J., Xu, S., Xu, S. and Liu, C.-Q.: Dynamics and fluxes of dissolved carbon under short-term
815 climate variabilities in headwaters of the Changjiang River, draining the Qinghai-Tibet Plateau, *J. Hydrol.*, 596, 126128,
816 doi:10.1016/j.jhydrol.2021.126128, 2021.

817 Zhou Y., Davidson, T. A., Yao, X., Zhang, Y., Jeppesen, E., de Souza, J. G., Wu, H., Shi, K. and Qin, B.: How autochthonous
818 dissolved organic matter responds to eutrophication and climate warming: Evidence from a cross-continental data analysis
819 and experiments, *Earth-Sci. Rev.*, 185, 928-937, doi:10.1016/j.earscirev.2018.08.013, 2018.

820 Zhou Y., Yao, X., Zhou, L., Zhao, Z., Wang, X., Jang, K. S., Tian, W., Zhang, Y., Podgorski, D. C., Spencer, R. G. M.,
821 Kothawala, D. N., Jeppesen, E. and Wu, F.: How hydrology and anthropogenic activity influence the molecular
822 composition and export of dissolved organic matter: Observations along a large river continuum, *Limnol. Oceanogr.*, 66,
823 1730-1742, doi:10.1002/lno.11716, 2021.